Synthesis of hydroxyapatite (HAp) and microwave assisted TiO_2-HAp composite coating on Commercially pure (CP)-Titanium for biomedical applications

Rahul Sarkar

Department of Biotechnology and Medical Engineering
National Institute of Technology Rourkela

Synthesis of hydroxyapatite (HAp) and microwave assisted TiO_2-HAp composite coating on Commercially pure (CP)-Titanium for biomedical applications

Thesis submitted in partial fulfillment

of the requirements of the degree of

Master of Technology

in

Biomedical Engineering

by

Rahul Sarkar

(Roll Number: 215BM1443)

under the supervision of

Prof. Arunachalam Thirugnanam

May, 2017

Department of Biotechnology and Medical Engineering

National Institute of Technology Rourkela

Biotechnology and Medical Engineering
National Institute of Technology Rourkela

Certificate of Examination

Roll Number: *215BM1443*

Name: *Rahul Sarkar*

Title of Dissertation: **Synthesis of hydroxyapatite(HAp) and microwave assisted TiO_2-HAp composite coating on Commercially pure (CP)-Titanium for biomedical application**

I, the below signed, after checking the dissertation mentioned above and the official record book (s) of the student, hereby state my approval of the dissertation submitted in partial fulfillment of the requirements for the degree of *Master of Technology* in *Biomedical Engineering* at *National Institute of Technology Rourkela*. I am satisfied with the volume, quality, correctness, and originality of the work.

Dr. A Thirugnanam

Supervisor

Biotechnology and Medical Engineering
National Institute of Technology Rourkela

Supervisor's Certificate

This is to certify that the work presented in this dissertation entitled "*Synthesis of hydroxyapatite (HAp) and microwave assisted TiO_2-HAp composite coating on Commercially pure (CP)-Titanium for biomedical applications*" by "*Rahul Sarkar*", Roll Number *215bm1443*, is a record of original research carried out by him under my supervision and guidance in partial fulfillment of the requirements of the degree of Master of Technology in Biomedical Engineering. Neither this dissertation nor any part of it has been submitted for any degree or diploma to any institute or university in India or abroad.

Supervisor's Signature

A. Thirugnanam

*This thesis is dedicated to my **Maa** and **Baba**, who instilled in me the virtue of perseverance and commitment and relentlessly encouraged me to strive for excellence.*

Acknowledgement

A project can never be completed without the help of a lot of people and the sound knowledge they provide in various aspects. The persons in the list that follow are the people who had some contribution for completing this project work.

First and foremost, I am deeply grateful for his valuable guidance, continuous support, insight, patience, and encouragement of my supervisor, **Dr. A. Thirugnanam**, without whose constant trust, gentle prodding, this project work would not have been completed.

I am indebted to the Department of Biotechnology & Medical Engineering for providing the necessary equipment & chemical supplies to fulfill this project. I also would like to thank the Head of the Department **Dr. Mukesh Gupta** for providing the platform for completion of this project work.

I am very grateful to Phd scholar **Mr. Shreeshan Jena** and **Ms. Chandrika Kumari** for their incessant support, inspiration and constructive criticism throughout my Project.

I would like to thank my batch-mate **Mr. Srijeeb Karmakar** and **Ms. Debadrita Paul** for giving their valuable time to assist me in the project.

I would like to thank all the technical assistant of NIT Rourkela for their technical support to carrying out the project.

Finally, I thank God and my loveable parents and family without them this would not possible. Their faith, support, and love for me are unbelievable, which gave me strength, motivation, and patience.

May 29, 2017
NIT Rourkela

Rahul Sarkar
(215bm1443)

Abstract

Hydroxyapatite (HAp) is an important bioceramic material widely used for many biomedical applications owing to its similarity to the inorganic composition of bone. Hydroxyapatite was synthesized by using wet precipitation method using calcium nitrate and diammonium hydrogen phosphate as a precursor. To maintain a constant pH, ammonium hydroxide solution was used. After synthesis, HAp samples were calcined at 850 °C and 1200 °C, for 2 hours, and allowed to cool at room temperature. The synthesized HAp and calcined HAp samples were characterized by X-ray diffraction (XRD), attenuated total reflectance-Fourier transform infrared spectroscopy (ATR-FTIR), scanning electron microscope (SEM), and transmission electron microscopy (TEM). Zeta potential test was performed and its values were found to be between -14.7 mV and -15.7 mV. The result inferred that hydroxyapatite particles would get precipitated in a short span of time and, not stable in colloidal solution. Dynamic light scattering (DLS) was also used to determine particle size distribution. The z-average diameter of particles was found to range from 400 nm to 457 nm. Transmission electron microscopy (TEM) result confirmed that calcined HAp (1200°C) has the largest particle size and synthesized HAp has the smallest particle size. After synthesis of HAp, microwave (MW) has been used as a substitutive method for HAp-based composite coatings on commercially pure (CP) titanium substrate. This is performed to enhance the bioactivity which is an important property for biomedical implants. The coating was made by microwave processing of CP-Ti packed in HAp at moderately higher microwave power. The composition of coating demonstrates TiO_2 as a major phase (which was formed due to oxidation) along with HAp as a minor phase. Synthesized HAp and calcined (850 °C) HAp coating on CP-Ti were performed and characterized. The XRD and SEM results confirmed the presence of TiO_2 and HAp on the CP-Ti specimens. The coated samples showed improved mechanical and biological performances. Microhardness of CP-Ti specimens increased after microwave processing, as the microhardness values of uncoated, synthesized HAp coated, and calcined (at 850 °C) HAp coated CP-Ti samples are 172.64 HV, 192.1 HV, and 192.45 HV respectively. Hence the studied showed that TiO_2-HAp coated CP-Ti specimens has significant potential in a biomedical application with improved bioactive properties.

Keywords: Hydroxyapatite (HAp), calcination, microwave processing, biological studies

Table of Contents

List of Figures

List of Tables

Chapter 1

Introduction

1.1 Background and significance of the study

Among all metallic implant material, titanium and its alloys (mostly Ti6Al4V alloy) have been successful for medical implant application because of corrosion resistance, higher strength to density ratio and biocompatible in nature [1]. When a material is inserted into a body, its surface is directly contact with cells, tissues and other biological materials. So, surface modification of titanium and its alloys has become more essential for osteo-integration and better biological performances [2]. That's why hydroxyapatite (HAp) has been introduced for coating purpose, which is bioactive, and osteoconductive in nature. As, inorganic material of a bone is similar to hydroxyapatite, coating with HAp has receives as a considerable attention. Such surface modification with hydroxyapatite could alter different properties of the surface [3-7].

A variety of coating techniques to coat HAp are available by either elevated temperature process (pulsed laser deposition, thermal spray etc) or lower-temperature process (electrophoretic, dip coating, biomimetic coatings etc) [8]. However, failure at the material coating interface leads to loosening of orthopaedic implants. To improve the adhesive strength of the coating, post coat heating treatment is required, which requires more time and cost [9]. Not only mechanical property of coating increases by incorporating another phase like titania (TiO_2), alumina (Al_2O_3), carbon nanotube (CNT) along with HAp, but also the biological properties such as bioactivity and osteo-integration.

Microwave (MW) processing of materials has an advantage of processing time reduction and saving energy. The mechanism of energy transfer is by the interaction of metal with electromagnetic (EM) field and is influenced by material's dielectric property. In this study, commercially pure (CP) Ti alloy has been coated with HAp by using the technique of microwave processing [10]. After coating of CP-Ti, *in vitro* studies were performed to evaluate biological performances.

1.2 Structure and properties of hydroxyapatite (HAp)

Hydroxyapatite is a highly valuable material for biomedical applications. It is a ceramic material, a special form of calcium phosphate. The structure of hydroxyapatite is

$Ca_{10}(PO_4)_6OH_2$, where as Ca/P ratio should be 1.67. The OH^- group of HAp can be replaced by other functional groups like F^-, Cl^-, and CO_3^- group. Bone has a similar inorganic composition as HAp. So, hydroxyapatite is a bioactive material, which will support bone tissue ingrowth, osteointegration used for orthopaedic and dental implant. HAp is a brittle material as it is ceramic in nature. HAp have drawn a great interest to researcher, as they are widely used as biomaterials, including such uses as coating on implant material, bone-tissue engineering scaffolds, bone fillers, repairing soft tissues and drug delivery system [11] because of their bioactivity, excellent biocompatibility, osteoconductive property and similar to bone inorganic compound. Hydroxyapatite also has a potential for cell targeting, labelling and can be act as a imaging and diagnosis material [12]. Also, HAp is considered as a model compound to mimic the biomineralization process [13].

Pure hydroxypatite is a stoichiometric HAp phase with a Ca/P molar ratio is 1.67 and it is the most stable form of calcium phosphate at normal temperature and varying pH. In preparation of HAp, aging and preparation kinetics are critical for the phase purity and chrystallographic structure of the product [14].

Most frequently, the crystal structure of HAp is hexagonal, lattice parameter is a = b = 9.432 Å, c = 6.881 Å and $\gamma = 120^\circ$. The chemical structure of HAp consists of an array of phosphate group (tetrahedral) held together by calcium ions. Hydroxyapatite can exists in another form, monoclinic with lattice parameters a = 9.4214 Å, b= 2a, c = 6.8824 Å, $\gamma = 120^\circ$. The arrangement of hydroxyl (OH^-) group is the major difference between the monoclinic and tetragonal form of HAp. In case of monoclinic, the adjacent OH^- groups are in same direction, where as in hexagonal structure, the adjacent OH^- groups are opposite direction [15]. The hexagonal HAp is generally formed during precipitation reaction of HAp at 25˚-100˚ C. The monoclinic HAp is formed by heat treatment of hexagonal form of HAp, this process is known as calcination. Human bone material is composed of non-stoichiometric nano-crystalline HAp with structural imperfections due to substituted with essential trace elements in crystal lattice [16]. Hydroxyapatite has two types of crystal planes, **a** and **b** planes considered as a positive charges and **c** planes considered as a negative charge. They accumulate opposite charge molecules. Therefore, a and b planes attracts acidic molecules, whereas c planes attracts basic molecules [17]. For HAp, pH value of a soaking medium plays an important role for charge accumulation. When HAp is immersed in a mineral acids or base, negative surface charge is generated of pH 5-8, upon increasing of pH more surface charge will observed [18].

The chemical composition, crystalline size, shape and their aggregation plays an important role for determining their properties and different biomedical applications. HAp as a nanoparticle has an excellent sintering ability, it also has a great bioactivity and higher reabsorbing property comparing to micro-scale HAp. Nano-HAp also can be used as a cell targeting, drug delivery and diagnosis applications [19]. In biomedical applications, the major strength of HAp is its biocompatibility and osteoconductive property.

1.3 Preparation of hydroxyapatite (HAp)

Synthesis of HAp can be prepared by various techniques reported in the literature, including sol-gel, wet precipitation, hydrothermal technique and biomimetic deposition. Synthesize of HAp is reported in mentioned literature as a **sol-gel method** [20], where as calcium nitrate tetrahydrate (CNT) were used as a calcium precursor and phosphoric acid (PA) were used as a phosphorous precursor. Ammonia was used to maintain pH in the range of 9-12. The schematic representation of the procedure is given in **Figure 1**. The concentration of CNT and PA was taken as such that should maintain Ca/P molar ratio approx. 1.67. Both the solute dissolved in distilled water, ammonia was added to PA solution followed by stirring in a magnetic stirrer. CNT solution was added drop by drop to PA solution, pH of the solution was maintained above 9 by adding ammonia. After 1 hr of rigorous stirring, solution was kept 24 hr for aging process. After aging process, the formed gel was dried in oven at 65˚C for 24 hr. After drying, powder obtained was washed in distilled water for two times to remove ammonium nitrate from the substrate. After that, calcination of powder was done at different temperature for 30 min soaking time using an electric furnace with a heating rate of 10˚C/min. It has been reported that, HAp samples prepared by sol-gel route are efficient to improve the contact and stability of the bone/implant interfaces in both *in vitro* and *in vivo* condition.

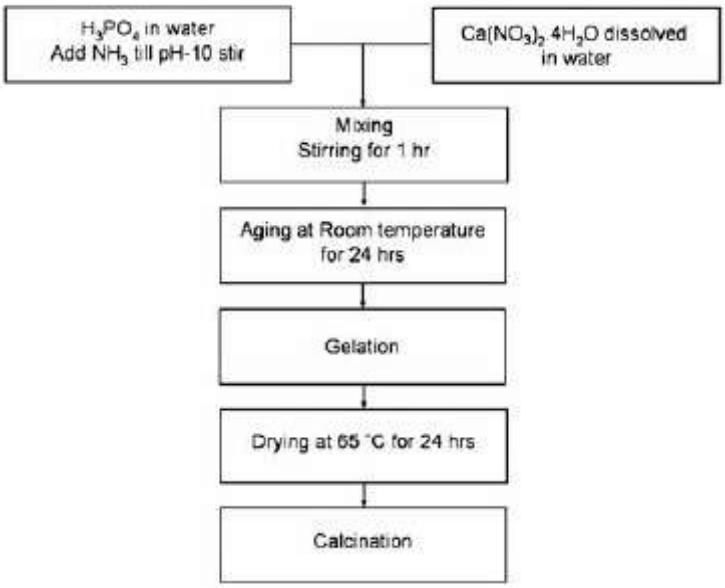

Figure 1. Experimental steps of preparation of HAp by sol-gel route

Hydroxyapatite also can be prepared by **wet chemical or wet precipitation method** [21]. **Figure 2.** represents experimental steps carried out in wet precipitation method. Calcium hydroxide was used as a calcium source and phosphoric acid was used a phosphate source. The precipitation reaction was first proposed by Yagai and Aoki. The precipitation reaction of HAp goes through the following equation :

$10\ Ca(OH)_2 + 6\ H_3PO_4 = Ca_{10}(PO_4)_6OH_2 + 18\ H_2O$.....(1)

Morphology, physical and chemical properties of produced hydroxyapatite is highly depends upon to the rate of addition of orthophosphoric acid. Addition of H_3PO_4 is directly linked with pH of the solution. The reaction temperature determines whether the sample is monocrystalline and polycrystalline. Preparation with lower temperature forms monocrystalline HAp, whereas at higher temperature polycrystalline HAp produced. Santos et al [22] proposed another reaction for producing HAp, where di-ammonium phosphate was used as a phosphate precursor and calcium hydroxide was used as a calcium precursor. Like the above reaction, pH of the reaction was maintained.

$10\ Ca(OH)_2 + 6\ (NH_4)_2.HPO_4 = Ca_{10}(PO_4)_6(OH)_2 + 6\ H_2O + 12\ NH_4OH$ …….(2)

$Ca(OH)_2 + 3\ Ca(H_2PO_4)2.H_2O = Ca_{10}(PO_4)_6(OH)_2 + 15\ H_2O$ …….(3)

Temperature was maintained above 40˚C, the higher temperature was used for enhancement of reaction kinetics of hydroxyapatite and to improve dissolution of calcium hydroxide. In wet precipitation method, Ca/P ratio = 1.67 was maintained. Another precipitation method was proposed, where calcium nitrate tetra hydrate was used as a calcium precursor and di-ammonium hydrogen phosphate was used as a phosphate precursor [23]. The grain size of HAp can be controlled by changing reaction time and temperature. Nano hydroxyapatite was produced by continue stirring of the precipitated solution at room temperature for 24 hr.

Hydrothermal technique for synthesizing ceramic materials was clearly considered as an essential technology and HAp can be synthesized by using this technique [24]. Hydrothermal synthesis is a process that utilizes single phase reaction by increasing temperature and pressure to crystallise ceramic materials directly from their solutions [24]. In hydrothermal process, Ca/ P molar ratio of HAp samples increases with increasing temperature and pressure [25]. HAp was also prepared by adding 2 gm of cetyl trimethyl ammonium bromide (CTAB) and the synthesis was conducted in an electric oven at 170˚C for two hours [26].

Biomimetic deposition technique was used for HAp synthesis. Stimulated body fluid (SBF) with same ion concentration of human blood plasma facilitates the nucleation and growth of hydroxyapatite particles. HAp was prepared by dissolving CNT and diammonium hydrogen phosphate in SBF at 37˚C [27]. SBF was prepared by according to Kokubos' method [28]. The apatite layer deposition on orthopaedic and dental implants promotes cell proliferation and differentiation on implant surface. Porous implants can be coated with hydroxyapatite by biomimetic deposition technique. The morphology, dissolution rate and interaction of HAp coating with SBF influenced osteogenecity and bone remodelling process. Hydroxyapatite coating was synthesized by **Electrodeposition technique**. Calcium nitrate and diammonium hydrogen phosphate was introduced as a calcium and phosphorous precursor and they were acts as electrolytes. For improving ionic strength, sodium nitrate was used. By applying constant anodic voltage, growth of hydroxyapatite induced [29]. HAp were synthesized by

using egg shell. At first, egg shell were collected and mechanically cleaned. After that it was calcined and followed by ball milling [30].

Figure 2. Experimental steps carried out in wet precipitation method

1.4 Hydroxyapatite (HAp) for biomedical applications

Hydroxyapatite has the potential for applications in bone and dental repair. In recent years, HAp is applied in drug delivery system, cell targeting, imaging, diagnosis etc. HAp is also used for rapid fractionalisation of nucleic acid, protein and antibodies. Due to same inorganic

composition of bone, HAp has been used for orthopaedics and dentistry for several years. HAp bioceramic material is used in powder for tooth and bone filling, as a particle for bone cement applications, used as unloaded implants, acts as a porous scaffold for temporary implants for bone in-growth and remodelling purpose, coating on metallic implant materials for increasing bioactivity and osteointegration, mechanical reinforcement in a polymer-ceramic bioactive composite [31-32]. For bone-tissue engineering, hydroxyapatite particles have been widely used. Nano/ microscale HAp promotes bone remodelling rather than HAp with smooth surface. HAp acts as a bioactive material in both *in vitro* and *in vivo* condition and the bioactivity influences upon the morphologies of HAp nanocystals.

HAp is considered as a potential candidate for scaffold material used in bone-tissue engineering applications, which act as a temporary candidate for cell growth, proliferation, differentiation and substitute bone-tissue regeneration after implantation. One of the major issues in this field is the development of fabrication techniques to tailor surface properties of HAp scaffolds in order to control and regulate cell biological responses. Furthermore, to better mimic the structure and function of native bone tissue, composite scaffolds are designed by dispersing HA particles in polymer matrix, in which HAp particles function as both bioactive and mechanical reinforcing components [31]. Kim et al. [32] have used PLGA/HAp composite scaffold to construct the living bone tissues.

Hydroxyapatite also has an application in soft tissue regeneration due to their outstanding biocompatibility with soft tissues such as skin, tendon, ligaments etc. The studies showed that HAp can activate fibroblasts and accumulate vessel endothelial cells and that support the healing of skin wounds [33]. The HAp composite products have been successfully developed for soft tissue augmentation, and a study demonstrated that HAp particles could stimulate the axonal out-growth, suggesting that HAp might provide a new approach for therapy or prevention of nervous injury [34].

HAp particle can serve as a carrier for protein/drug delivery and gene therapy due to their excellent biocompatibility, physiochemical properties (size, morphology, and surface composition) low toxicity, low production cost, excellent storage stability, inertia to microbial degradation, and pH dependent dissolution etc. pH is a prime factor for degradation of HAp particles. The degradation of HAp particles increases when pH changes from alkaline to acidic, which accelerates the release of drug molecules from HAp surface. This concept is useful in drug delivery in the tumour region [35].

1.5 Titanium (Ti) as biomaterials

The metallic implant biomaterials majorly divided into four sub-groups : the stainless steels, the cobalt based alloys, titanium metals and miscellaneous others. Titanium material is extracted by Kroll's process. The lightness of titanium, corrosion resistance, excellent biocompatibility and good mechanochemical properties are salient features for biomedical implant application [36]. This stimulated the needs of creating orthopaedic implants. The total hip joint prosthesis has shown in **Figure 3.** [37]. More clinicians, material scientists, and

biomedical device design engineer favours titanium and its alloy based biomaterials for implant purposes than other two major groups of metallic implant materials such as cobalt-chromium alloy and stainless steel. The four commercially pure (CP) Ti grades, Ti-6Al-4V alloys were the first titanium biomaterials used for implants. The chemical compositions of above two titanium material are given in **Table 1-2** [36].

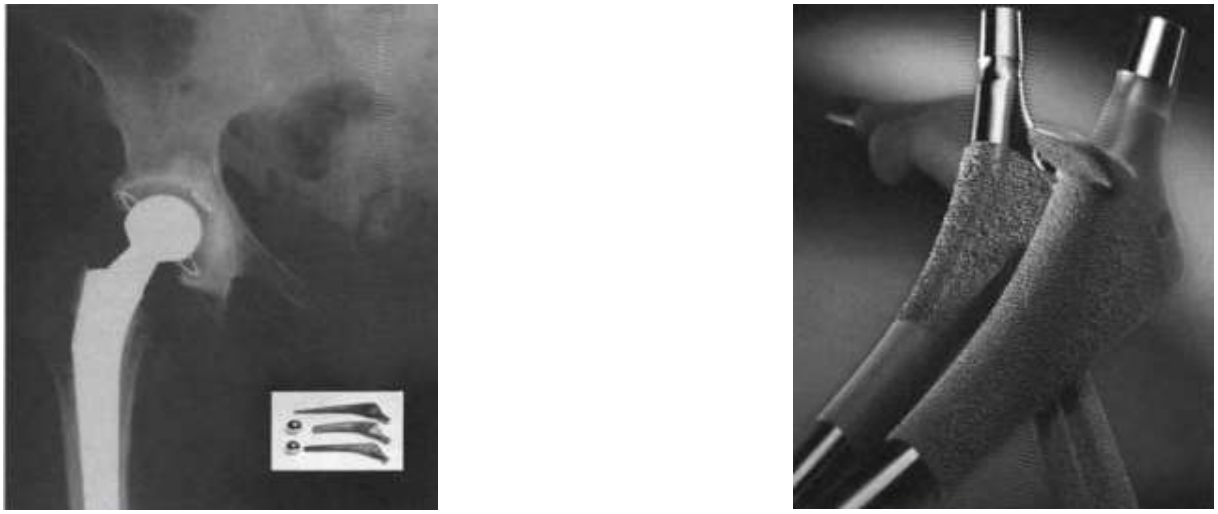

Figure 3. Titanium hip joint prosthesis

Table 1. Chemical compositions of CP-Ti of different grades

Element	Grade 1	Grade 2	Grade 3	Grade 4
N	0.03	0.03	0.05	0.05
C	0.10	0.10	0.10	0.10
H	0.015	0.015	0.015	0.015
Fe	0.20	0.30	0.30	0.50
O	0.18	0.25	0.35	0.40
Ti		Balance		

Table 2. Chemical compostions of Ti-6Al-4V alloys

Element	Wrought, forging (F136, F620)	Casting (F1108)	Coating (F1580)
N	0.05	0.05	0.05
C	0.08	0.10	0.08
H	0.012	0.015	0.015
Fe	0.25	0.30	0.30
O	0.13	0.20	0.20
Cu	–	–	0.10
Sn	–	–	0.10
Al	5.5–6.50	5.5–6.75	5.50–6.75
V	3.5–4.5	3.5–4.5	3.50–4.50
Ti		Balance	

Titanium is exists as a hexagonal close-packed (HCP) structure (α-Ti) up to 882˚C and a body-centered cubic (BCC) structure (β-Ti) above that temperature. By the addition of alloying elements, titanium enables to change wide range of properties:

1. Aluminium is known as α stabilizer, that is, transformation temperature from α to β phase increases.
2. Vanadium is known as β stabilizer, that is, transformation temperature from α to β phase decreases.

Commercially pure titanium grade and its alloys with α stabilizing element maintain their hcp crystal structures at room temperature, and they are classified as **α Ti grades**. They have single phase microstructure, which provides good weldability. These grades exhibits good higher temperature creep properties and they are used in cryogenic application because they do not exhibit ductile-brittle transformation. These alloys cannot be heat treated single phased, strengthening effect of α alloys are achieved by precipitation hardening process.

Alpha-beta titanium alloys have the combination of both α and β stabilizers that are typically used in biomedical applications where both characteristics are desired. Alpha-beta titanium alloys, has high tensile strength, good creep resistance, and it can be strengthen by heat treatment.

Most **beta titanium alloys** contains small amount of α stabilizers which permits second phase strengthening to high levels at room temperature. β titanium can be cold formable, as bcc phase of β Ti alloy is ductile. β alloys are prone to ductile-brittle transformation, that's why it is not used in cryogenic applications. Because of hot and cold working properties of beta alloys, effort has been devoted to create specialized β Ti alloys for medical applications.

1.6 Hydroxyapatite (HAp) coating on titanium implant

In the biomedical engineering field, the aim of coating or surface modification is to promote biocompatibility, while at the same time inhibiting wear and reducing corrosion. It has been seen that surface coating and modifications offer improvements in both clinical reliability

and performance of the components by modifying its property. At present, coating techniques such as dip coating, electrophoretic deposition, sputter process, thermal spraying, and sol-gel have been used to apply ceramic coatings. However, each suffers from disadvantages that prevent it from ideal coating system (**Table 3**) [37]. HAp coated implants have been demonstrated to show extensive bone apposition in animal models. The biological interactions of released calcium and phosphate ions lead to the development of good interfacial strength between implant and bone. HAp coated implant shows faster healing property and improved attachment to the bone material. Quality and performance of implant depends on diverse factors such as the thickness, porosity, composition, crytallinity of the coating, surface roughness, biomechanical functional loading and total development of the device. Furthermore, the chemistry and surface topography of HAp deposited as thin films on implants are known to accelerate bone formation and increase the strength of bone-implant interface.

During the process of preparing HAp coating via any physical and chemical process, a number of factors can influence the characteristics of the resultant coating. To guarantee a stable coating, the substrate is typically a surface treatment before coating. The intermediate oxide layer, TiO_2 is designed to enhance the bonding between Ti and HAp and thus integrating of the coating.

Table 3. Advantages, drawbacks and thickness of different coating techniques

Coating technique	Advantages	Drawbacks	Coating thickness
Electrochemical deposition	Low cost, coat complex shapes, rapid, uniform coating thickness	The bonding strength between coating and substrate is not strong enough	0.05–0.5 mm
Electrophoretic deposition	Coat complex shapes, rapid, uniform coating thickness	Difficult to produce a crack-free coating	0.1–2 mm
Plasma coating	Low cost, high deposition rate	High temperature induces thermal decomposition, line of sight technique, amorphous coating due to rapid cooling	30–200 μm
Pulse laser deposition	Coating by crystalline and amorphous phases, both porous and dense coating	Line of sight technique, low deposition rate, expensive	0.05–5 μm
Sol–gel nanocoating	High purity, homogeneous, no residual stresses, complex shapes can be easily coated	Edge cracking might occur, cannot induce mechanical interlock, post-treatment needed (curing)	50–400 nm
Sputter coating	Dense and uniform coating thickness on flat surface	Amorphous coating, line of sight technique, time-consuming, low deposition rate, expensive	0.5–3 μm

1.7 Microwave processing

Now a days, microwave used in material processing. However, the actual heating mechanism by microwave irradiation is less understood. Many popular heating such as dipolar heating and conduction heating have been mostly explored. Heating mechanism involved during interaction of microwave to different materials in different manner. Interaction of microwave with different characteristic materials – metals, non-metals and composites (metal matrix composites, ceramic matrix composites and polymer matrix composites) have been discussed using suitable explanation [38]. Uniform heating occurs by microwave processing unlike normal heating technique by furnace.

Microwaves are electromagnetic (EM) waves consists of an electric and magnetic field. Both the fields are orthogonal to each other with wavelengths in the range of 1-1000 mm. Microwaves are converted to heat energy depending on the type of interaction with targeted materials. The microwave processing depends upon dielectric and magnetic property of a material. The electric field and magnetic field of microwave interacted with dielectric molecules of a material [39-40]. Microwave gain popularity in food processing, whereas polar molecules are trapped by microwave irradiation such as water, fat, and resulting uniform heating of an element. In last several years, microwave processing has been used in versatile applications such as synthesis and drying applications, sintering applications and materials processing, and coating applications. It is clear from the above mentioned statement is that, in recent years, the interest in uses of microwave energy is slowly getting shifted from food processing toward processing of advanced materials in the recent years. These material processing applications involve different ranges of temperature depending upon the interaction of microwave with material. During microwave material interaction electromagnetic fields of microwaves have important role in heat generation at the atomic level, that's why uniform heating produced by microwave heating. The material properties ultimately determine the effect of the EM field on the materials in terms of energy absorption characteristics. Consequently, the actual mechanism of microwave material interaction and relations of material properties with electromagnetic characteristics of microwave are prime factor in microwave processing. Here, in this study, microwave was used for coating HAp on commercially pure titanium surface.

Literature Review

Siddharthan et al. [10] used microwave as a coating purpose on commercially pure titanium (CP-Ti). During microwave heating, oxygen got dissolute in Ti surface, and titanium oxide (TiO_2) layer formed on CP-Ti surface. Hydroxyapatite particles were covered on the titanium surface, during microwave processing, titanium oxide sintering along with hydroxyapatite due to microwave absorption of non-stoichiometric titanium dioxide. Finally,

the coating was in composite nature, and that was confirmed by XRD analysis. Pre-treatment is much needed before microwave processing, after pre-treatment microwave processing was done at 800 W microwave power. In this particular study, microwave (MW) processing time varies on CP-Ti materials in *in situ* condition. Microwave processing for 22 minute was the optimum condition for composite coating on Ti surface. The author claimed that, formed titanium dioxide is non-stoichiometric in nature due to limited presence of oxygen. A study on bad gap energy of TiO_2 was carried out to confirm non-stoichiometry of titanium oxide. Composite coated sample possesses better response in bioactivity studies. Osteoblast cell culture was also done on processed CP-Ti surface, cell adherence was seen under FESEM microscope.

Hydroxyapatite (HAp) is a bioceramic material and same inorganic composition of bone. Hydroxyapatite was synthesized according to the protocol [23]. Various parameter affects for preparation of hydroxyapatite. Wet chemical precipitation technique has practical advantages such as simplicity of experimental process, less reaction temperature, and possibility of controlling chemical composition and morphology of final product with harmless bi-product. Therefore in this study, HA powders were synthesized by the wet chemical precipitation technique where calcium hydroxide $Ca(OH)_2$ was used as the calcium source precursor while orthophosphoric acid (H_3PO_4) as the phosphorus source precursor. There are several factors -such as the pH value of the reaction solution, dropping rate of the acid solution into the alkaline solution, temperature of the reaction solution, the stirring rate, etc.- that play role in the wet chemical precipitation process and some of these parameters were investigated in this work [41].

Each of these factors individually may influence the crystal and/or amorphous phases that are obtained at the end of the process. Preparation and reaction of the precursor solutions, aging of the final solution and precipitation, filtrating and washing, drying and eventually heat treating the precipitation are the main steps that were carried out throughout the synthesis process. HAp has a tendency to agglomerate and this was confirmed by SEM. Ca/P ratio is the main criteria for preparing HAp.

The effect of sintering temperature on the properties of HAp was discussed by Muralithran et al. [42]. The physicochemical properties of hyroxyapatite is largely depends on thermal treatment during synthesis process. The sintering behaviour of a material is achieved by calcination of HAp samples. It is concerned with the effects of grain size of the sample on the physical properties such as relative density and hardness. The thermal stability of HAp affects in terms of phases present, densification behaviour and hardness. How to porosity and grain size depends upon hardness of sintered HAp was also investigated. The relation between hardness and grain size was correlated. It is suggested that a certain critical grain size phenomenon was influencing the hardness of HA ceramics i.e. above this critical grain size, the hardness would decrease as a result of grain growth.

The mechanical properties of sintered HAp depends on the sintering temperature was discussed [43]. The microstructure and mechanical properties of sintered HAp depends on

the sintering temperature of HAp sample. HAp particles were prepared by the wet precipitation method and its purity and degree of crystallinity were investigated via XRD. Calcined HAp powder was produced by heating the sample in an electric furnace at elevated temperature. Elastic moduli of the specimens have been measured by ultrasonic pulse echo method; compression strengths were measured on the Instron testing machine. Micro-structural information has been derived from the elastic moduli measurement and then verified by analysis of photomicrographs of shatters. It is observed that the average shape of pores transforms from strongly oblate to round at higher sintering temperatures. This transformation leads, in particular, to increased strength of the material since the stress concentration near pores is reduced. The HA nanopowders were prepared by precipitation and were systematically investigated as a function of temperature from 80°C up to 900°C [44]. High purity HAp are obtained at low temperature and HA structure is main- tained up to 900°C. The HAp with lower crystallinity shows needle-like shape particles with a low surface area value, whereas the HAp with higher crystallinity has rod shape particles. The increase in crystalline size with temperature takes place by the growth of the particles in uniaxial direction.

The particle size of HAp increases due to calcination, and it is well justified by the classical nucleation-growth-agglomeration mechanism. In the proposed model, the mechanism of formation of HAp particles starts with a phase called nucleation, followed by the aggregation of supercritical nuclei ruled by surface energy excess, which counterbalance the repulsive forces between particles. The aggregated-agglomerated particles formed solid bridges, and the formed agglomerated HAp continue to grow as distinct particles due to repulsive forces between particles [45]. Due to calcination, diffusion starts between two HAp particles, and that results nucleation and growth. That's why particle sizes of HAp increased after calcination.

The stability of HAp in a colloidal suspension is determined by zeta potential measurement. Zeta potential is a measurement of a potential difference of an electric double layer. When particle moves in a solution, ions within the electric double layer boundary moves with it, and this boundary is also called the slipping plane. The electrokinetic potential exists at the boundary is known as zeta potential of the sample in a particular solution [46]. For zeta potential measurement, pH is an important factor. The zeta potential vs pH curve will always positive at low pH and negative at high pH level. In the zeta potential vs pH plot, when the plot pass through zero zeta potential is known as **Isoelectric point**. Generally colloidal suspension is least stable at isoelectric point. Zeta potential value higher than 30 mV is considered as stable suspension. The value of zeta potential of particle is obtained by Henry equation. The zeta potential of a particle depends upon strength of the electric field gradient, dielectric constant, and viscosity of the medium.

Dynamic light scattering (DLS) used for measuring particle sizes of nanoparticles. Hydrodynamic radius (R_H) of a particle was measured by DLS, so, actual particle sizes of the sample couldn't estimated by this technique. R_H of a solid spherical particle can be

derived by Stokes- Einstein equation [47]. According to Stokes-Einstein equation, DLS measurement depends upon diffusion coefficient, viscosity of the medium, and temperature of the colloidal suspension.

Objectives

- Synthesis of hydroxyapatite (HAp) by wet precipitation method.
- Comparative study of synthesized HAp with calcined HAp by XRD, FTIR, TEM, SEM, zeta potential and DLS.
- Microwave processing of titania-HAp composite coating on commercially pure titanium.
- Evaluation of mechanical and biological performance of coated CP-Ti specimens.

Chapter 2

Methodology

2.1 Preparation of hydroxyapatite

To prepare HAp via wet chemical method, diammonium hydrogen phosphate ($(NH_4)_2HPO_4$) and calcium nitrate tetra hydrate ($Ca(NO_3)_2 \cdot 4H_2O$) were used as precursors of phosphate and calcium. The experimental steps of HAp preparation was drawn in **Figure 4**.

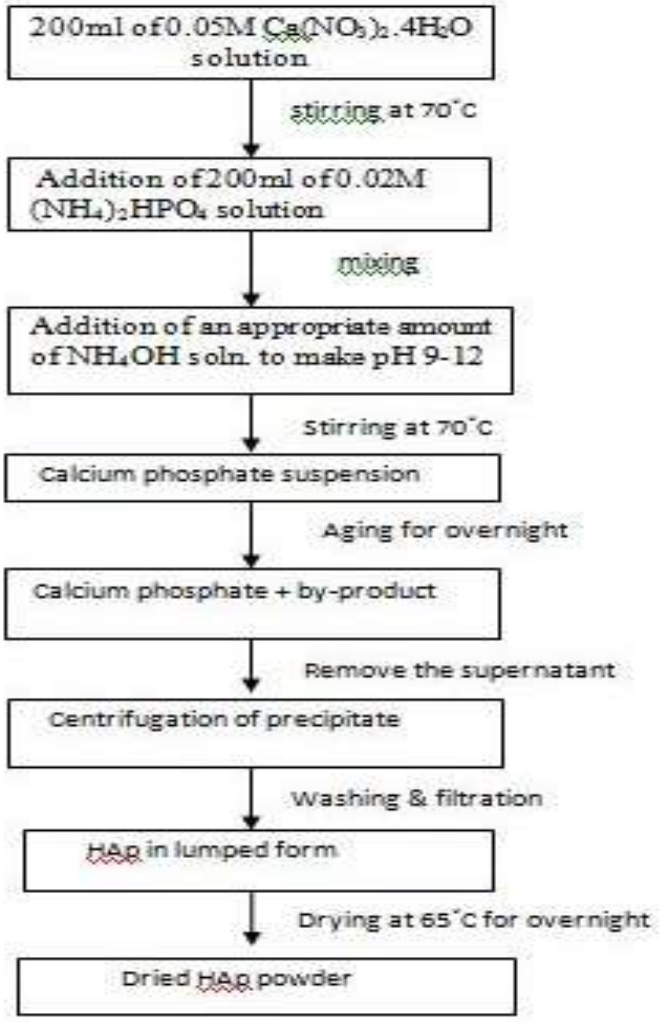

Figure 4. Flowchart of experimental preparation of HAp

Distilled water was used to prepare all the solutions. The desired Ca/P molar ratio should be maintained of =1.67. Ammonium hydroxide (NH_4OH) was added to maintained pH of the solution 9 to 12. The following chemical reaction takes places during the synthesis of HAp:

$10Ca(NO_3)_2.4H_2O + 6(NH_4)_2HPO_4 + 8NH_4OH \rightarrow Ca_{10}(PO_4)_6OH_2 + 20NH_4NO_3 + 11H_2O$ (4)

0.03M diammonium phosphate solution was added to 0.05M calcium nitrate at a drip rate of one drop per second at 65 °C temperature. Calcium nitrate solution was put in a magnetic stirrer at the time of addition of diammonium hydrogen phosphate solution. After addition, the solution was left overnight for the aging process. Supernatant formed after aging and it was removed from the precipitate. Then, the achieved precipitate was separated from the liquid phase by centrifugation followed by washing of the sample with distilled water. After that, the precipitate was oven-dried at 65°C overnight to form a powder. The above-mentioned samples were then characterized using various techniques.

2.2 Calcination

In the calcination process, 0.2gm of synthesized HAp sample was placed in an open alumina crucible and then heated in an electric furnace to eliminate moisture from the sample, improving degree of crystallinity. Two samples were heated at a temperature of 850°C and 1200°C for 2 hours at a heating rate of 3°C/min and afterward cooled slowly to room temperature. **Figure 5.** is the image of electric furnace used for calcinations.

Figure 5. Image of the electric furnace used for calcinations

2.3 Zeta potential analysis of synthesised and calcined HAp

The zeta potential (ZP) is also termed as electrokinetic potential. It is the potential difference of a colloid particle at the slipping plane moving under an electric field. The electrokinetic potential of a surface is the amount of work needed to bring a unit positive charge from infinity to the surface with constant velocity. The ZP reflects the potential difference

between the layer of EDL (electric double layer) of electrophoretically mobile particles and dispersant particles around them at the slipping plane. Zeta potential (Malvern Instruments, US) was done for synthesized as well as calcined HAp sample. Here, dispersed media was distilled water dilution was performed. The concentration of HAp in distilled water solution was 1mg/100ml. Before the ZP measurement was carried out, the solution was ultrasonicated for 10 min in a probe sonicator to disperse the particles within the solution. Two ml of the sonicated solution was then moved into a plastic disposable cuvette and placed inside the sample holder. The ZP test was done for three HAp samples (One synthesized and two calcined HAp samples).

2.4 Dynamic Light Scattering (DLS) of HAp

DLS is a technique that can be used to determine the size distribution profile of small particles (nano scale). Basically, in DLS, hydrodynamic radius (R_H) of a particle is measured. So, it is not a confirmatory test to determine particle size of a sample. Dynamic light scattering (DLS) is a areas of colloidal chemistry. Hydrodynamic radius of particle is measured by using Stokes-Einstein equation. DLS particle size measurements were performed for both synthesized and calcined HAp particles using a High-Performance Particle Sizer (Malvern Instruments,US) to obtain mean intensity particle sizes of the corresponding samples.

1 mg of HAp was added into 100 ml of distilled water and the solution was continuously stirring by magnetic stirrer. Then, 10 ml of solution was taken out from that solution for DLS. Before the DLS measurement was performed, the solution was ultrasonicated for 10 min in a probe sonicator in order to disperse the particles within the solution. One ml of the ultasonicated solution was then transferred into a plastic disposable cuvette and placed inside the sample holder. The DLS measurement was done for three HAp samples as stated earlier.

2.5 Microwave assisted coating of CP-Ti

Before microwave processing on CP-Ti, pre-treatment of all the samples were done by the following technique. The CP Ti metal sample (7 mm×7 mm×1 mm) was polished by emery paper of grade 1, grade 2, grade 3 and grade 4 respectively. Then, etching of the sample was done by Kroll's reagent (in 25 ml solution, 23 ml distilled water, 1.5 ml conc. nitric acid and 0.5 ml hydrofluoric acid is used).

A cup-shaped crucible made out of alumina was used. Alumina was used as a microwave absorbent, which absorbs electromagnetic radiation. During microwave processing, at first crucible got heated, then it transfers to alumina, from alumina to hydroxyapatite powder titanium samples got heated. The sample placement inside the crucible for microwave processing in represents in **Figure 6**. Enhancement of heating has been done by alumina powder. The dimensions of the crucible were: diameter of 55mm, the height of 45 mm with

a crucible wall thickness of 6 mm. The metal sample was placed inside a crucible in a manner such that it was covered with HAp powder and then alumina powder as two distinct layers. The thickness of HAp layer to alumina layer was 1: 5. For avoiding direct contact between crucible and microwave plate, crucible was placed in a petriplate with maintaining some distance between microwave glass and plate. The microwave (MW) processing was carried out using a domestic microwave oven (SAMSUNG, 2.45 GHz, 900 W power). The MW processing was carried out for 20 min at lower microwave power (180 W) for initial heating and equilibrium. Subsequently, processing at 900 W was carried out for 15 min.

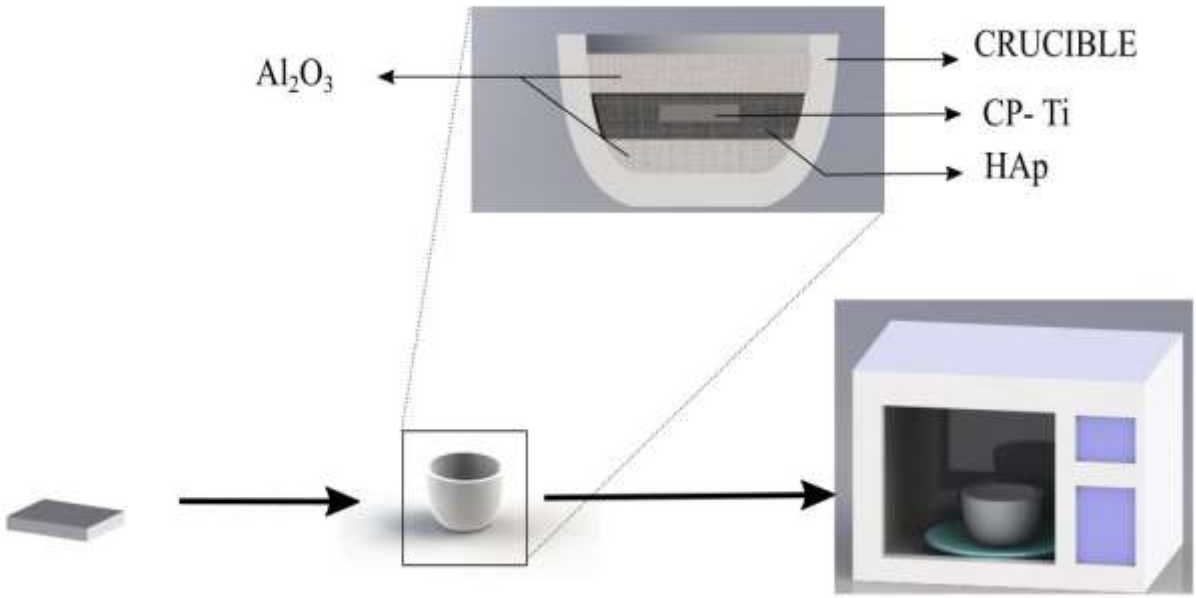

Figure 6. Placement of CP-Ti sample inside the crucible for microwave processing

2.6 Characterization

The synthesized HAp was analyzed for phase identification by X-ray diffraction (XRD) study with Cu Kα radiation (Rigaku, Ultima IV). To determine the functional groups present in synthesized HAp, Fourier transform infrared (FTIR) spectroscopy (Bruker, Alpha FTIR spectrometer) was performed over the range of 500 to 4000 cm^{-1}. After calcination, a comparative study of phase evolution has been carried out by XRD. Comparative study of functional group analysis was done by FTIR. The synthesized and coated HAp samples were characterized by scanning electron microscope (SEM). Chemical compositions of all HAp samples were determined by energy dispersive spectroscopy (EDS). The uncoated and coated samples were also analyzed for phase evolution by XRD. The surface morphology and chemical composition of coated samples were examined under the scanning electron microscope (SEM) (JEOL JSM 6480LV, USA) in secondary electron imaging mode at 20 KV and EDS. The conformation of composite nature of coating of CP-Ti was done by XRD

and SEM analysis. Morphology and crystal structure of calcined (850°C) HAp was measured by transmission electron microscopy (TEM).

2.7 Micro-hardness testing

The resistance to indentation of a material is known as hardness. Micro-hardness is incorporated where 'macro' hardness test is not usable. The term micro-hardness testing usually refers to static indentations made by load of 1kgf or less. Here, Vickers hardness test was used to determine hardness of a commercially pure titanium material (according to ASTM standard). The unit of hardness in Vickers hardness test is represented as HV. A square-based pyramid diamond indenter was used.
Here, a load of 500 gf and dwelling time of 15 second was applied to all CP-Ti samples. We can represent it by 500HV15. Four hardness values (HV) were calculated at four different locations for each sample. All tests have been done is duplicates.

2.8 Protein adsorption studies

The protein adsorption studies were performed by soaking the CP-Ti specimens in protein solution (1 mg/ml BSA in phosphate buffer saline (PBS)), and subsequently incubating them at 37 °C for 24 h. The specimens were removed after 24 h and the solution was centrifuged at 4000 rpm for 10 min. The quantitative analysis of protein adsorption of different CP-Ti samples was executed by using the Bradford assay. An aliquot 100 µl of the non-adsorbed protein solution was mixed with 1 ml of Bradford reagent and 2 ml of distilled water and kept in dark for 10 min. After that, the absorbance was determined by UV spectrophotometer measurement at 595 nm. All measurements were performed in duplicates for each time.

2.9 Hemocompatibility studies

The hemocompatibility studies were performed by immersing the specimens in 10 ml of physiological saline (0.9% w/v) in test tubes and incubating for 24 h. Goat blood (20 ml) was mixed with sodium citrate (1 ml, 1 mg/ml) and was further diluted with physiological saline (v/v;8:10). Diluted blood (0.5 ml) was added into each test tube and kept at 37 °C for 1 h. For positive control, 0.5 ml of blood was added to 0.5 ml of 0.01 N HCl and 10 ml of physiological saline. For negative control, 0.5 ml of blood was added to 10 ml of physiological saline. After incubation, the specimens were centrifuged at 6000 rpm for 10 min. The absorbance (OD) was recorded at 545 nm. Measurements were performed in duplicates for each specimen. The percentage (%) hemolysis was calculated using the following equation.

$$\%\ hemolysis = \frac{OD_{test} - OD_{negative}}{OD_{positive} - OD_{negative}} \qquad (5)$$

3.0 Bioactivity studies

The bone bonding ability of a substrate is evaluated by investigating the apatite formation on its surface immersed in stimulated body fluid (SBF) with same ion concentration of human blood plasma. The *in vitro* bioactivity was evaluated by immersing the specimen in SBF. The SBF is prepared according to the protocol suggested by Kokubo and Takadama [28]. The specimens were immersed in SBF maintained at 37°C in a constant temperature water bath for 21 days. After that, the specimens were removed, and then rinsed with distilled water. The specimens were dried at 37°C for 12 h before observation under SEM (NOVA, NANOSEM 450) in secondary electron imaging mode at 10kV and magnification of 5,000X to study the apatite growth on different titanium samples.

3.1 Cell viability study

The cell viability assay was carried out using MG 63 osteoblast cell lines. The osteoblast cells were cultured in Dulbecco's Modified Eagle's Medium (DMEM) supplemented with 10% FBS and penicillin-streptomycin. The specimens were sterilized using UV treatment for 20 min. each prior to cell seeding. The CP-Ti specimens (triplicates) were placed in a culture plate and incubated with culture medium for 3 h in a humidified incubator at a constant temperature of 37°C with 5% CO_2. After incubation, the cells (5×10^4 cells) were seeded dropwise on the specimens and incubated for 2 days in order to allow attachment of cells to the specimen surface. After incubation, the specimens were washed twice with PBS and incubated with fresh culture medium containing 20 µl MTT solution (5 mg/ml) at 37°C for 4 h. After removal of the MTT solution, 1 ml of dimethyl sulphoxide (DMSO) was added to each well plate to dissolve the formazan crystals. The absorbance of this solution was quantified by UV spectrophotometer (double beam spectrometer 2203, SYSTRONICS, India) at 595 nm.

Chapter 3

Results and discussion

4.1 Characterization of HAp and coated samples

4.1.1 Comparative study of XRD of synthesized HAp and calcined HAp

The conformation of hydroxyapatite by phase evolution was indicated by X-ray diffraction. All major peaks of HAp were seen. Data were collected in the 2θ range of 20°–60°, with a step size of 0.05°, and scan rate of 5°/min. **Figure 7.**Shows the X - ray diffraction patterns of synthesized as well as calcined HAp samples. All XRD patterns show diffraction lines characteristic of HAp as seen in JCPDS standards (9-432) and literature. We can observed from the diffraction pattern of all HAp samples that the peaks becomes more sharper for calcined HAp samples rather than synthesized HAp samples. When the temperature was increased, the hydroxyapatite peaks became sharper, due to crystal growth. Also we can estimated from the diffraction patterns that the full width half maximum (FWHM) of major peaks of calcined HAp sample are smaller than synthesized HAp sample, and has shown the same trend upon higher calcination temperature. According to Scherrer's formula, FWHM is inversely proportional to crystallite size of the samples. So, particle size of HAp samples goes increasing after calcination. So, particle size of HAp samples increased from 850°C to 1200°C calcination temperature. We can infer from XRD analysis, degree of crystallinity of HAp samples increases due to calcination.

4.1.2 Functional group analysis of synthesized HAp

FTIR analysis of HAp samples were done in the wavenumber range from 4000cm^{-} to 500cm^{-} (**Figure 8.**)**.** Absorption peaks for Phosphate ($PO4^{3-}$) and hydroxide (OH^{-}) groups of HAP were seen in the FT-IR spectra. The formation of hydroxyapatite was denoted by the broad asymmetric phosphate band centred from about 1000-1100 cm^{-1} with symmetric phosphate bands at 957 cm^{-1}, which corresponded to the $PO4^{3-}$ ion. Major peaks for the phosphate group were between 1100 cm−1 to 960 cm−1.

The bands assigned to the stretching modes of hydroxyl groups in hydroxyapatite were seen at 3567 cm^{-1}, 629cm^{-1}. Also a low intense band of absorbed water (stretching) was present in the spectrum of synthesized HAp (**Figure 8(a)**). Both calcined HAp spectrum, stretching of water were not seen. So, after calcination, samples become more anhydrous. Sharpest stretching has been found in 1200°C calcined HAp (**Figure 8(c)**). We can infer from that, degree of crystallinity is increased after calcination.

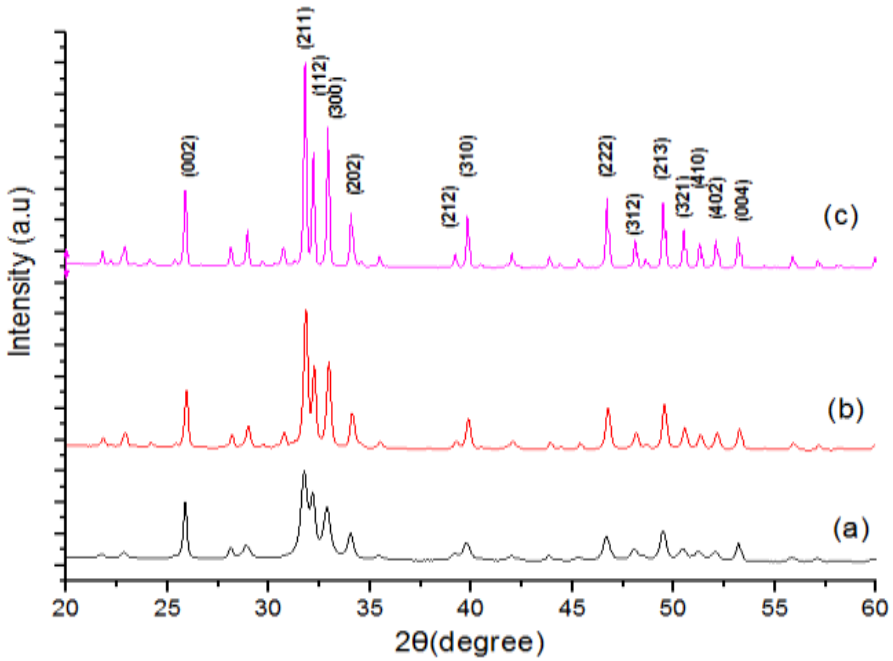

Figure 7. XRD patterns of (a) synthesized HAp (b) calcined HAp at 850°C and (c) calcined HAp at 1200°C

4.1.3 Transmission electron microscopy analysis of calcined (850°C) HAp

Figure 9, 10, 11, and 12 Shows the TEM analysis results of the calcined HAp (850°C) sample. The bright field and dark field image of calcined HAp sample was shown in fig. 10(a) and 10 (b) respectively. Due to calcination, hydroxyapatite particles are in aggregated form. Spherical shaped as well as rod shaped HAp particles were seen in TEM images. Particle sizes were measured manually in fig. 11, and the results showed that near about 100 nm sizes of particles were present in the sample. So, it can be expected that, synthesized HAp samples were formed as a nanoparticle. By high-resolution TEM (HRTEM), a detailed crystal structure of HAp has been studied, as shown in fig. 12(a). The HRTEM analysis revealed lattice fringes, and it is called the d-spacing of the planes. The distance of the lattice fringes corresponding to the plane is 0.34 nm. It represents the crystallinity of HAp . The lattice defects are identified as dark narrow lines as a differentiator in between the illuminated patches and the patches having parallel lines on it. Patches are said to be the Moiré patterns usually formed due to some misaligned identical lattices. Selected area energy dispersive (SAED) pattern as shown in Fig. 12(b), the plane represents polycrystalline material. Scanning transmission electron microscopy (STEM) analysis was done for evaluating elemental distribution of hydroxyapatite particles. It is a qualitative analysis and position of O, Ca and P elements were seen in STEM images represented in different colours (fig. 13).

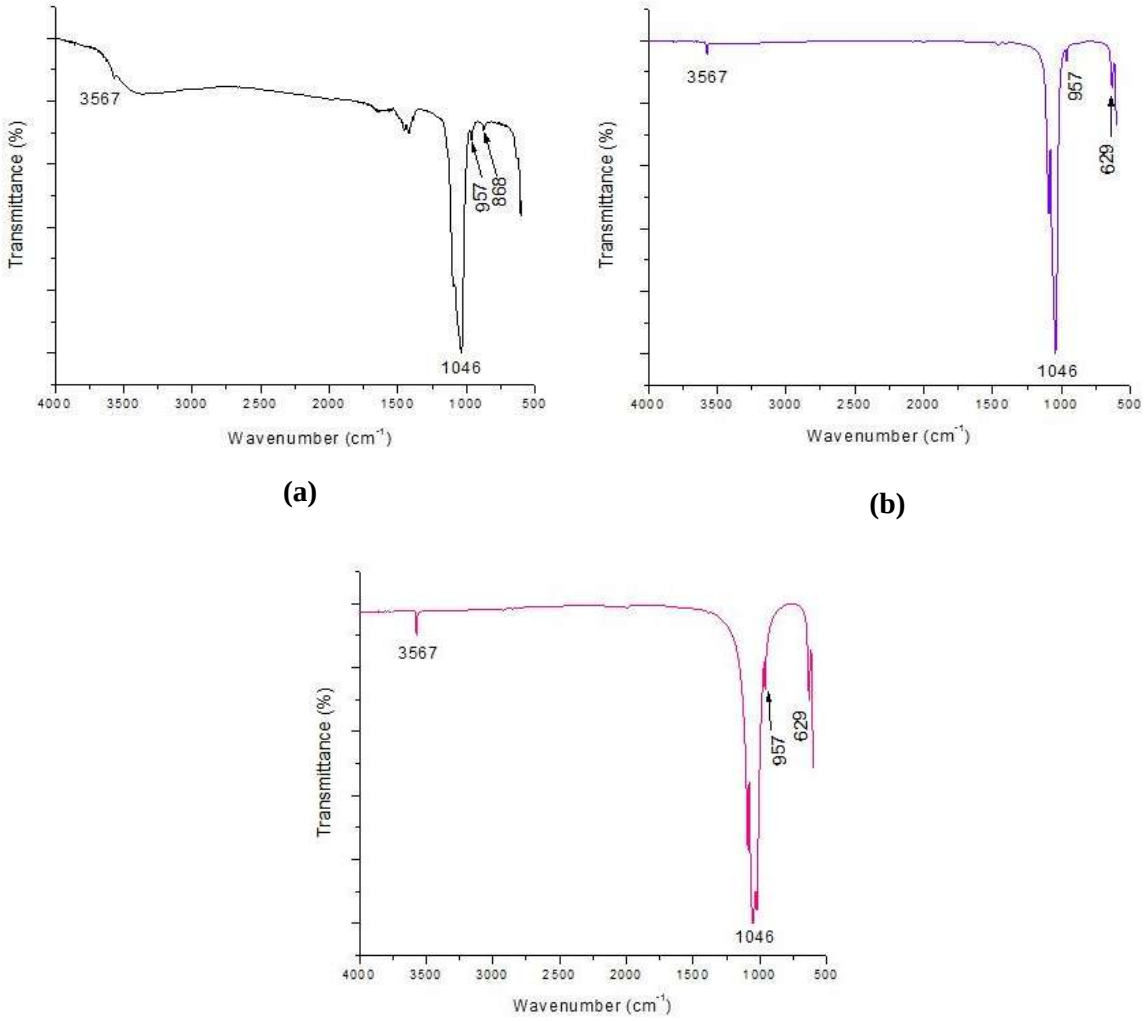

Figure 8. FTIR spectrum of (a) synthesized HAp (b) calcined HAp at 850°C and (c) calcined HAp at 1200°C

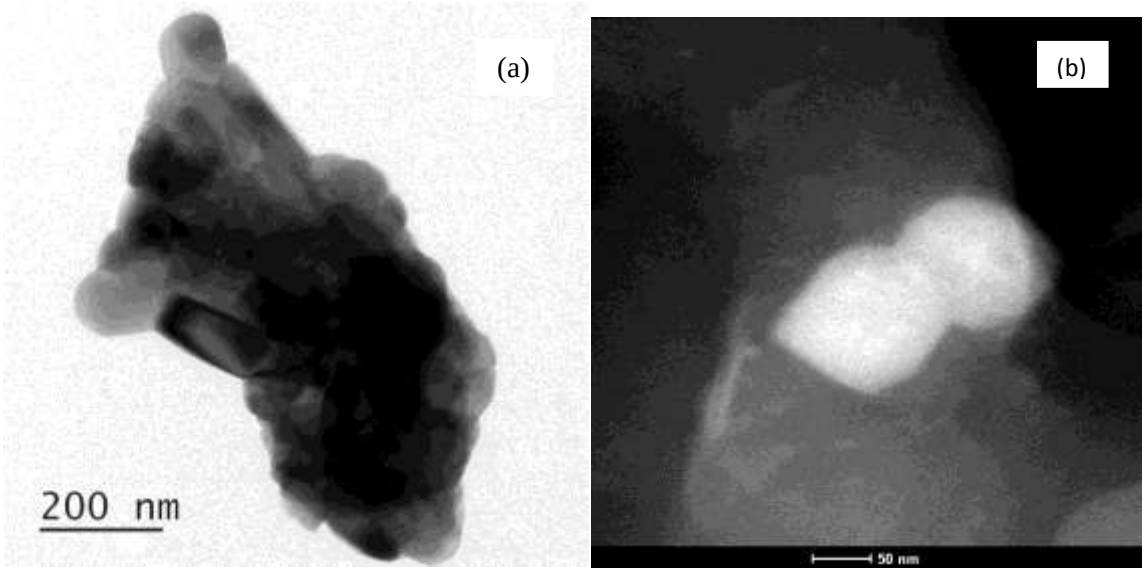

Figure 9. Bright field and (b) Dark field image of calcined HAp

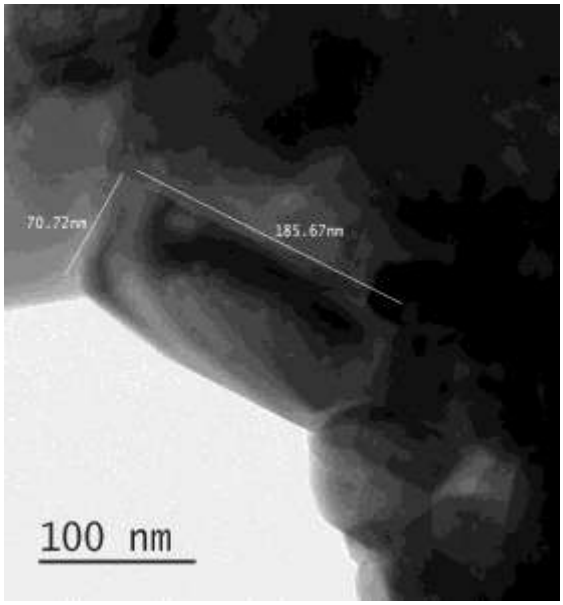

(a)

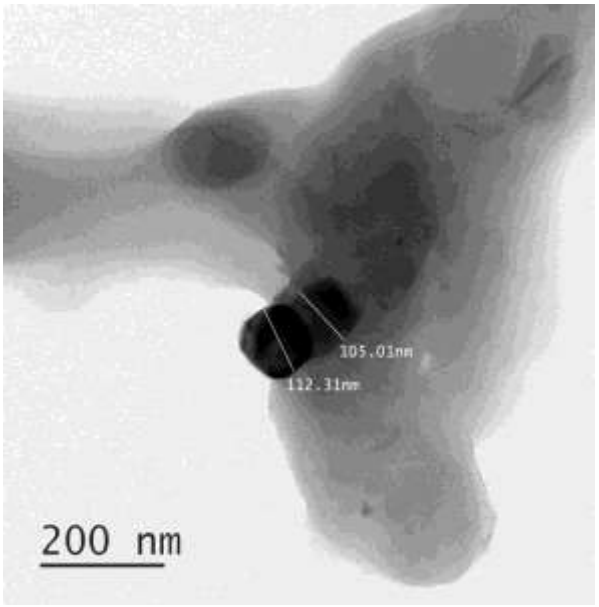

(b)

Figure 10. Particle size measurement of (a) rod shaped HAp, and (b) spherical shaped HAp

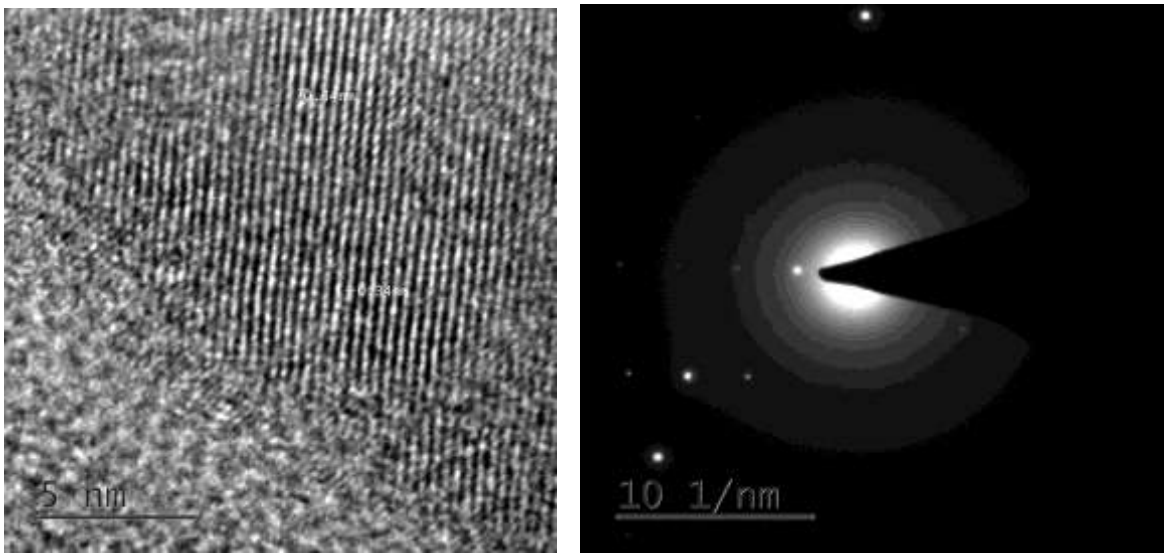

Figure 11. (a) HRTEM image, and (b) SAED patter of HAp

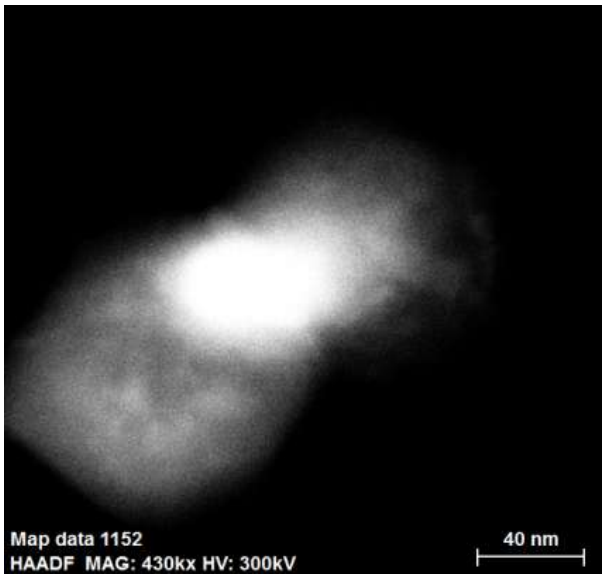

(a)

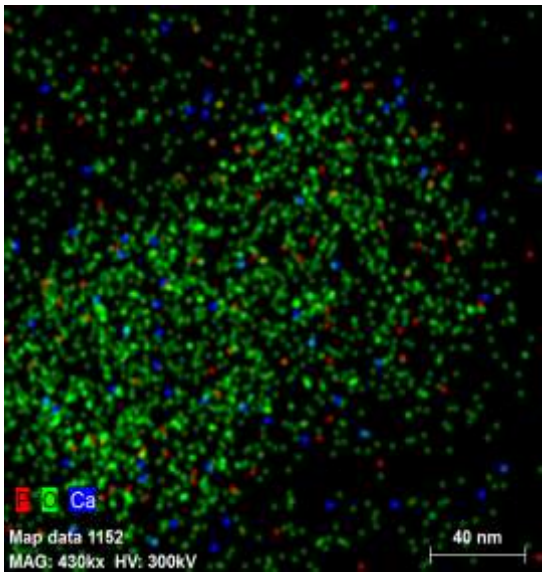

(b)

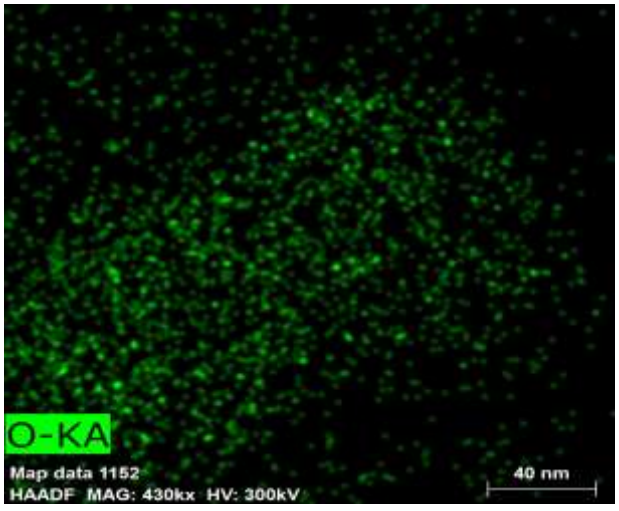

(c)

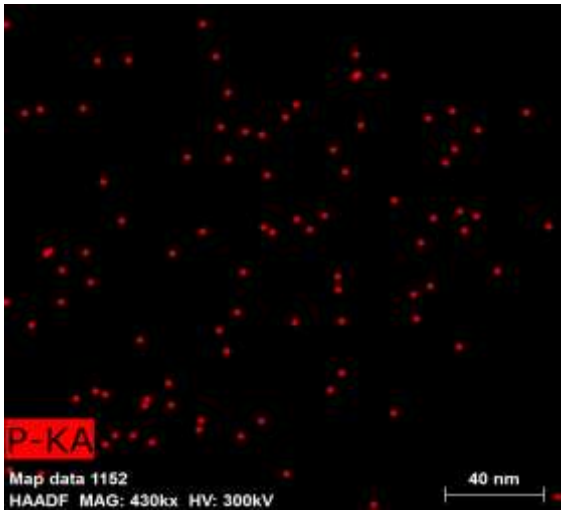

(d)

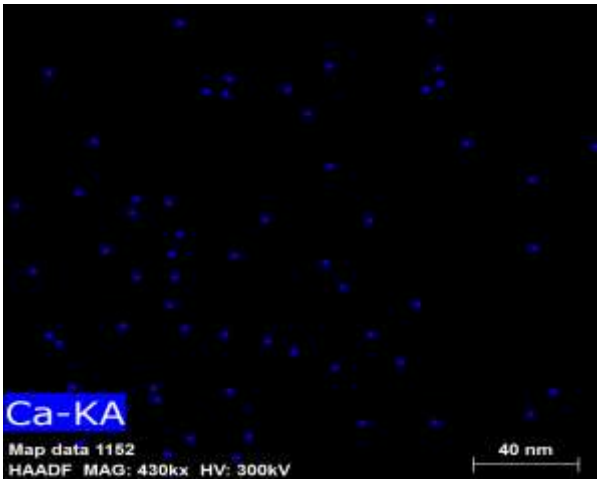

(e)

Figure 12. Elemental distribution of HAp by STEM analysis

4.1.4 Confirmation of phases on CP Ti samples after coating through microwave processing

The XRD patterns of the CP-Ti sample before microwave processing and after microwave processing were represented in **Figure. 13(a) and (b)**. The microwave processed sample showed peaks corresponding to rutile (TiO_2) and hydroxyapatite phase. The microwave processing resulted in a composite nature of coating of titania and apatite as seen from XRD studies. The titania–HAp coatings obtained an advantage over pure HA coating. Due to formation of titanium oxide layer, mechanical performances of titanium will be altered. It is observed from literature that this titania surface modification shows enhancement in osteoblast adhesion and cell growth. To identify HAp diffraction peak on CP-Ti, slow scan of coated sample was done with a range of 25˚ to 35˚ angle (**Figure 13(c)**).

4.1.5 Morphology of HAp samples

The surface morphology of synthesized HAp and calcined HAp samples in **Figure 14, 15.** and **16.** were examined under SEM. Morphology changes of Hydroxyapatite particles were observed due to increase in temperature. Calcined samples have shown nearly uniform structure rather than synthesized HAp. Crystallinity of HAp was increased due to calcination. Increasing temperature affects the particle sizes of the samples. 1200°C and 850°C calcined HAp samples has a higher particle sizes than synthesized HAp samples.

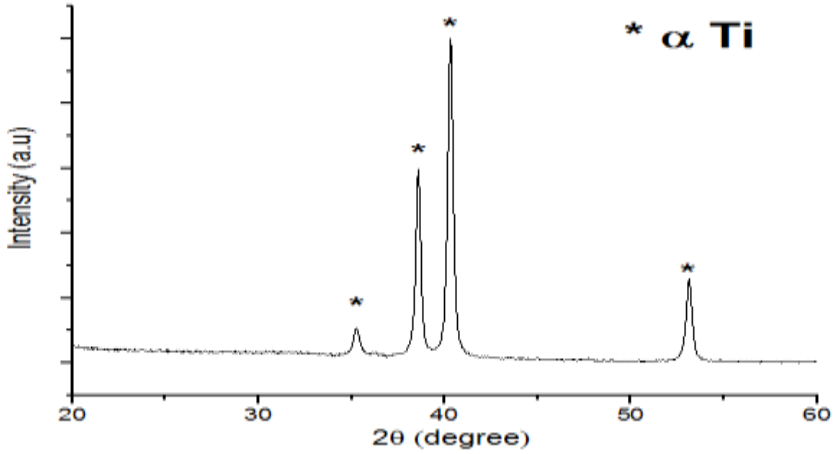
* α Ti
Intensity (a.u)
2θ (degree)
20
30
40
50
60

(a)

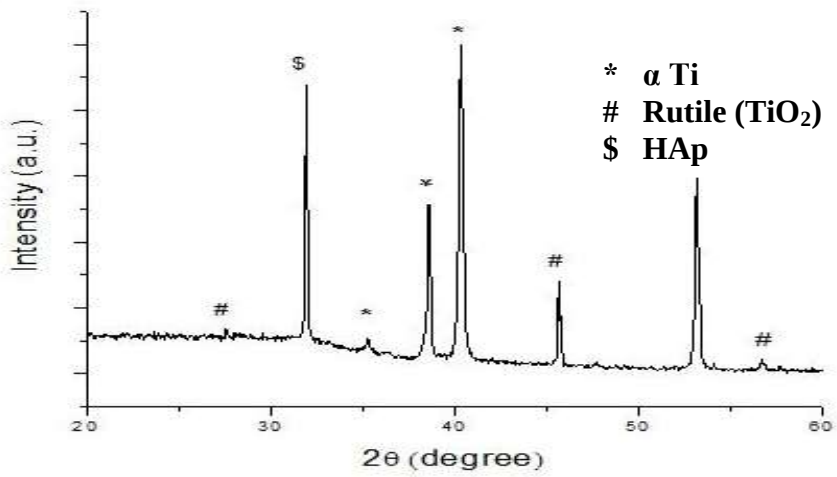
* α Ti
# Rutile (TiO2)
$ HAp
Intensity (a.u.)
2θ (degree)
20
30
40
50
60

(b)

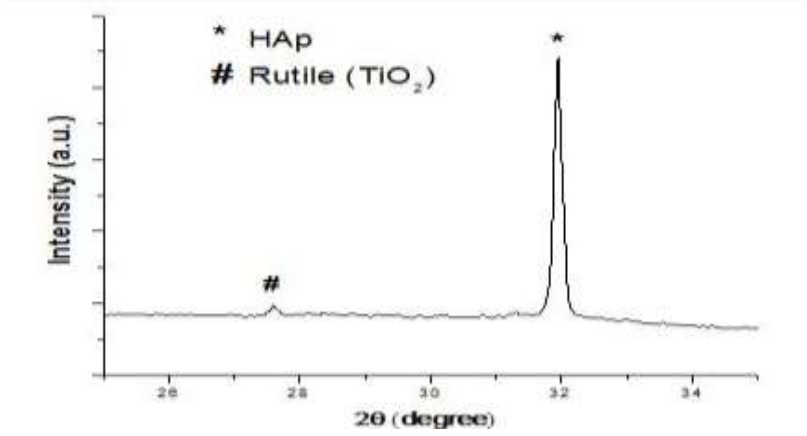
* HAp
# Rutile (TiO2)
Intensity (a.u.)
2θ (degree)
26
28
30
32
34

(c)

Figure 13. XRD patterns of (a) uncoated CP-Ti and (b) Synthesized HAp coated CP-Ti specimens after microwave processing (c) synthesized HAp coated CP-Ti with slow scan to identify apatite peaks

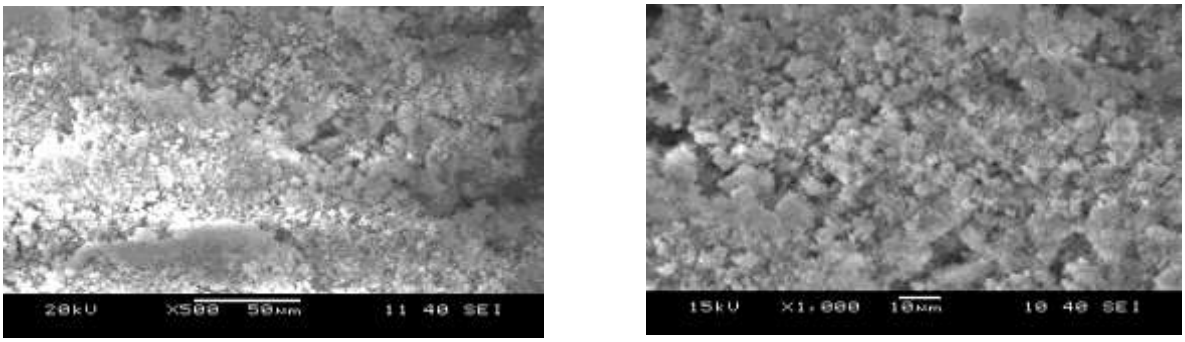

(a) (b)

Figure 14. XRD patterns of (a) uncoated CP-Ti and (b) Synthesized HAp coated CP-Ti specimens after microwave processing (c) synthesized HAp coated CP-Ti with slow scan to identify apatite peaks

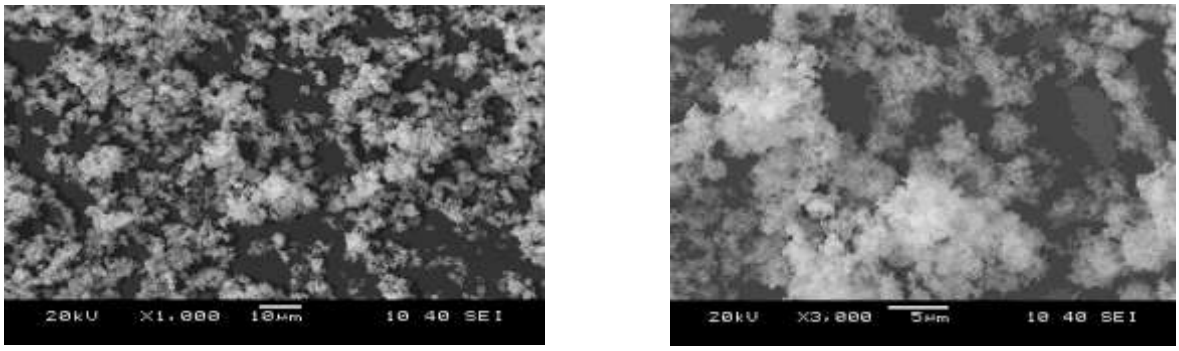

(a) (b)

Figure 15. SEM micrograph of calcined (850°C) HAp in (a) X1000 and (b) X3000 magnification

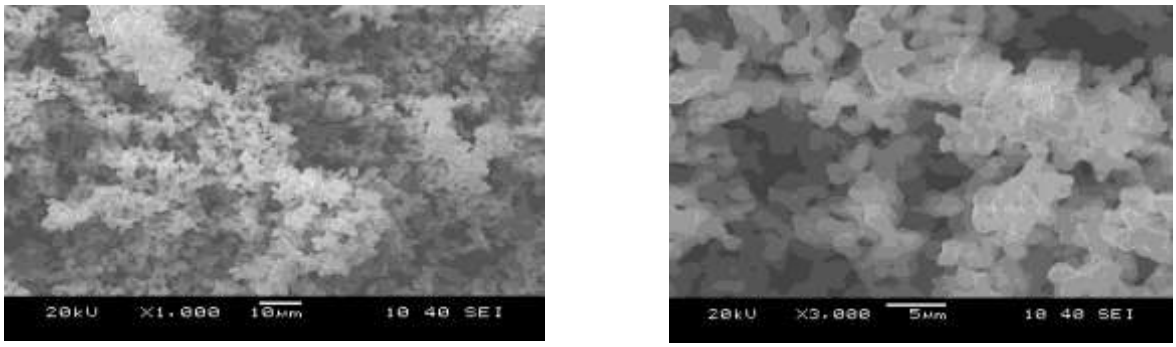

(a) (b)

Figure 16. SEM micrograph of calcined (1200°C) HAp in (a) X1000 and (b) X3000 magnification

4.1.6 Energy Dispersive Spectroscopy (EDS) of HAp samples

EDS is an analytical technique used for analysis of elements present in the sample and composition of a sample. **Figure 17 (a), (b)** and **(c)** represents the EDS spectra data for

synthesized HAp, 850°C calcined HAp and 1200°C calcined HAp respectively. Based on EDS data, the Ca/P weight ratio for derived HAp was calculated and was found to be 1.92, 1.70 and 1.88 for synthesized HAp, 850°C calcined HAp and 1200°C calcined HAp respectively. The desired Ca/P ratio was almost maintained for 850°C calcined HAp, so 850°C calcined HAp was chosen for coating on CP-Ti rather than 1200°C calcined HAp sample. Ca/P weight ratio of the derived HAp samples at different temperatures show considerable difference. It can be inferred that Ca/P weight ratio is dependent of calcination temperature.

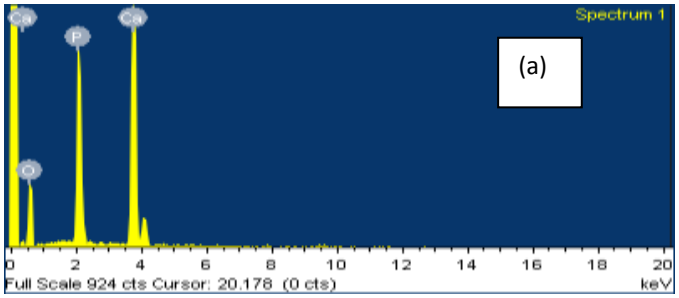

Elements	Wt %	At %
O	47.35	67.18
P	18.06	13.24
Ca	34.59	19.59

Ca/P ratio = 1.92

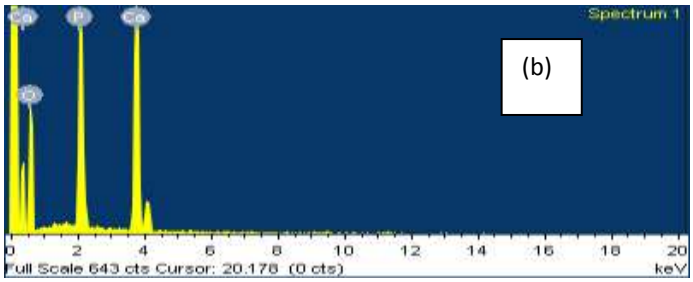

Elements	Wt%	At%
O	58.87	76.38
P	15.21	10.19
Ca	25.92	13.43

Ca/P ratio = 1.70

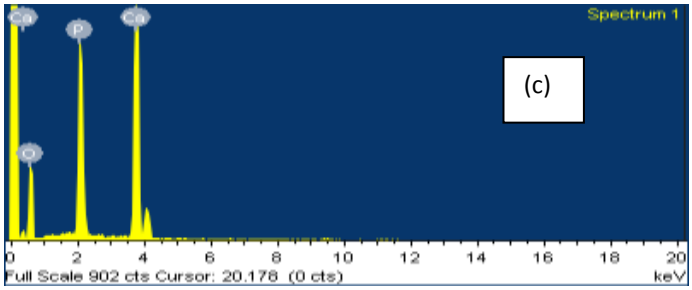

Elements	Wt %	At %
O	50.25	69.66
P	17.27	12.36
Ca	32.48	17.96

Ca/P ratio = 1.88

Figure 17. EDS results of (a) synthesized HAp, (b) 850°C calcined HAp, and (c) 1200°C calcined HAp

4.1.7 Morphology and EDS analysis of coated sample

The SEM micrograph shows (**Figure 18. and 19**.) a growth of oxide layer around particles for synthesized and calcined HAp coated samples. Hydroxyapatite particles were seen on the top surfaces of the coating samples and that was confirmed by EDS (**Figure 20 and 21**.).

The composition of coating elements such as O, Ca, and P were present on the surface of the CP-Ti sample and was confirmed by EDS analysis.. The SEM study also indicates the composite nature of coatings comprising of rutile and HAp. The growth of oxide scales and sintering of HAp was presumably due to microwave absorbing property of titanium dioxide resulting permanent composite coating. Elemental composition and their atomic and weight percentage were shown in the following tables.

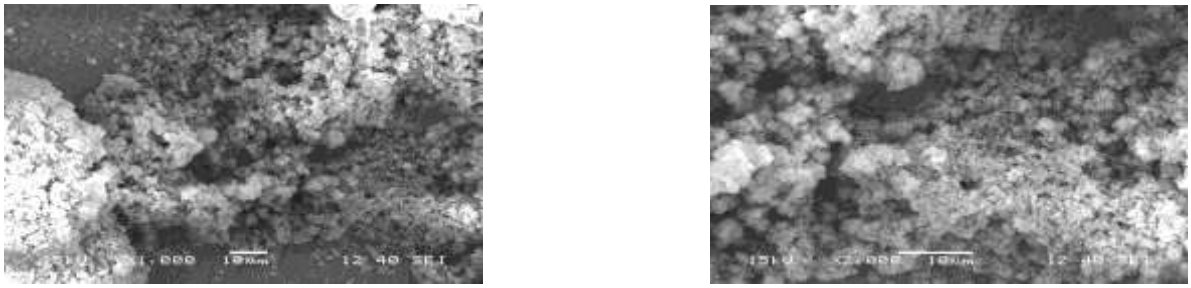

(a) (b)

Figure 18. SEM micrograph of synthesized HAp coated CP-Ti sample in (a) X1000 and (b) X2000 magnification

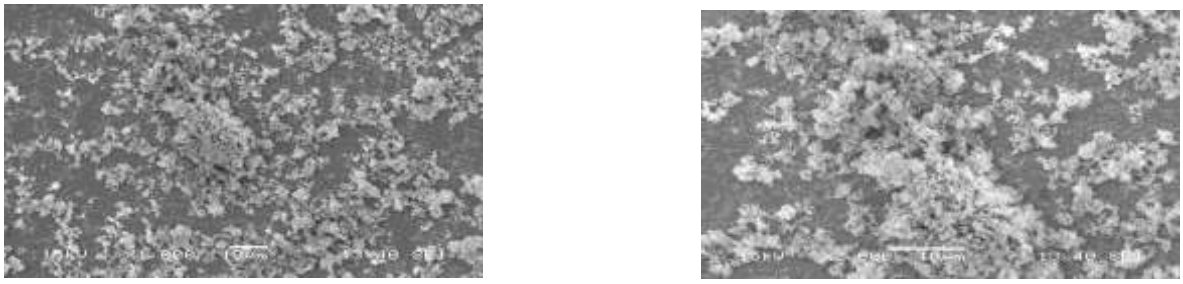

(a) (b)

Figure 19. SEM micrograph of calcined HAp (850°C) coated CP-Ti sample in (a) X1000 and (b) X2000 magnification

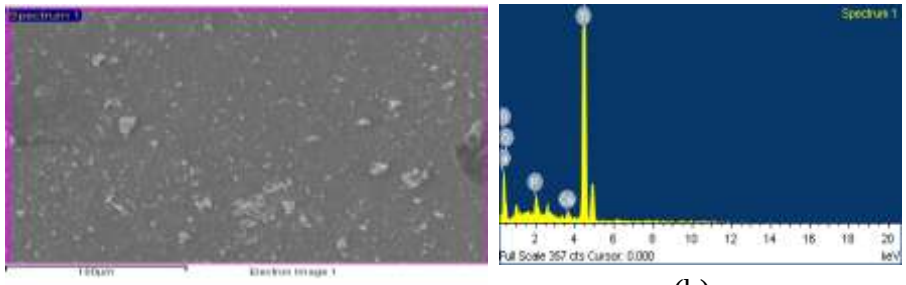

(a) (b)

Elements	Wt %	At %
O	20.90	43.94
P	1.08	1.11
Ca	0.60	0.50
Ti	77.42	54.38

Figure 20. EDS spectrum and composition of the selected region of the synthesized HAp coated CP-Ti sample

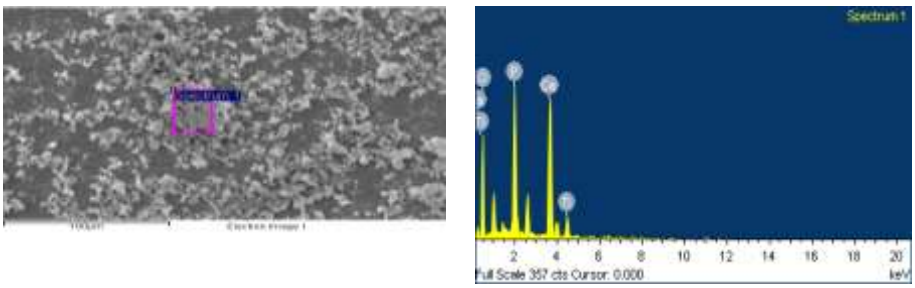

Elements	Wt %	At %
O	61.48.	78.64
P	13.80	9.12
Ca	20.25	10.34
Ti	4.47	1.91

Figure 21. EDS spectrum of the selected region of the calcined HAp(850C) coated CP-Ti sample

4.2 Visualisation of surface charge of HAp

The zeta potential of HAp particles was successfully measured as shown in **Figure 22(a), (b)** and **(c).** All the examined particles exhibit a negative zeta potential of around −14mV to -16 mV. Synthesized HAp, Calcined HAp at 850°C and Calcined HAp at 1200°C has a zeta potential value -14.7 mV, -14.9 mV and -15.7 mV respectively. It is observed that zeta potential value increases slightly with heat treatment. Generally, it is seen that a more negative zeta potential is favourable for adsorption of extracellular matrix and attachment of the bone cells.

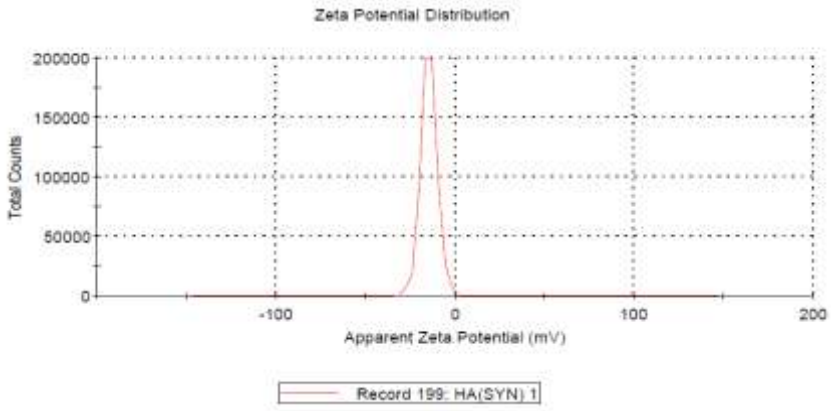

(a)

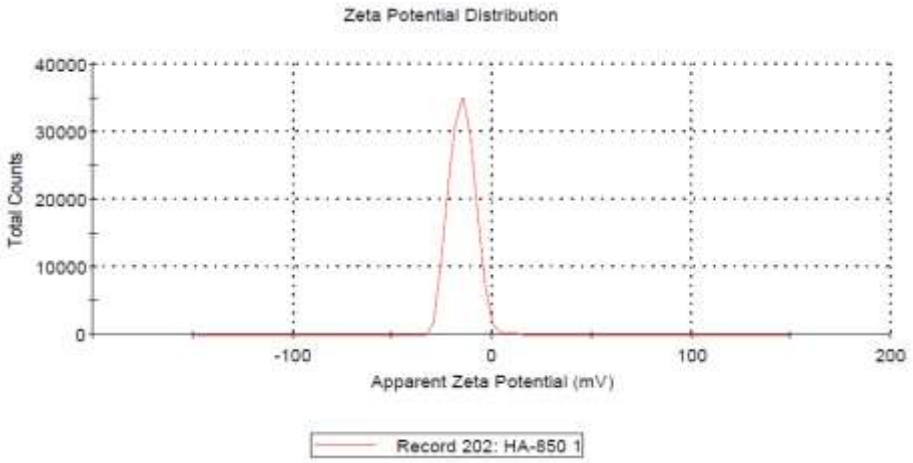

(b)

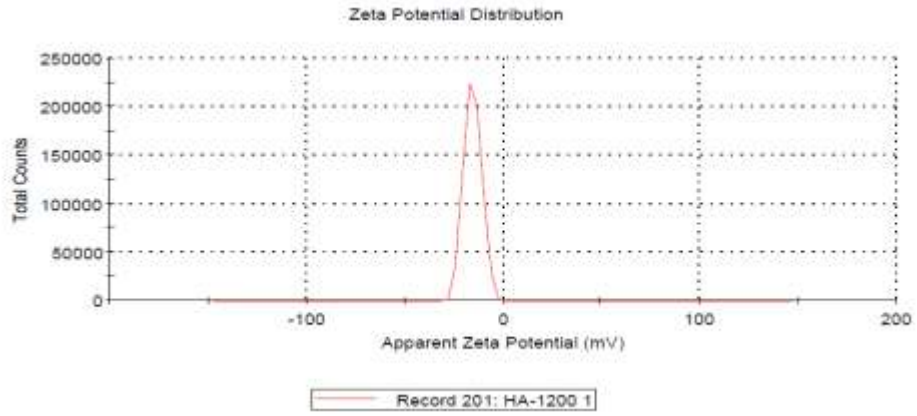

Figure 22. Zeta potential plot of (a) Synthesized HAp (b) calcined HAp at 850°C and (c) calcined HAp at 1200°C

4.3 Effect of heat treatment on particle size distribution

Particle size measurement by DLS was carried for all HAp samples. There is a change in hydrodynamic radius in HAp due to heat treatment. DLS measurement shows the z-average diameter of all HAp samples are in between 400 nm-457 nm. **Figure 23(a), (b)** and **(c)** represent the plot of particle sizes of all HAp samples with respect to intensity. Lowest z-average diameter is for synthesized HAp sample (400.5 nm) and highest is for 1200°C calcined HAp sample (457.1 nm). So, due to calcinations, particle sizes of HAp samples increases. Z-average diameter for 850°C calcined HAp sample is 434.3 nm.

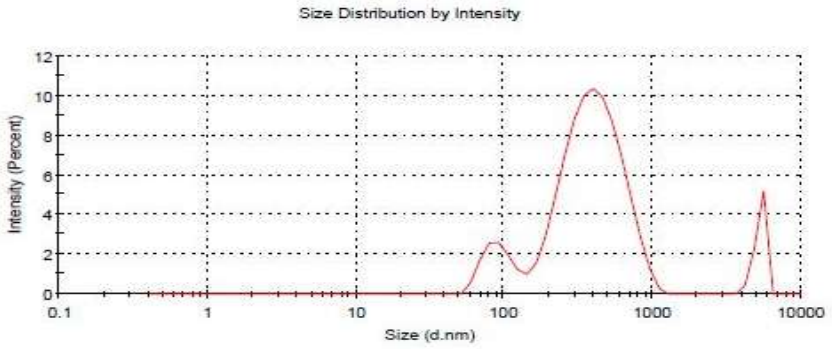

(a)

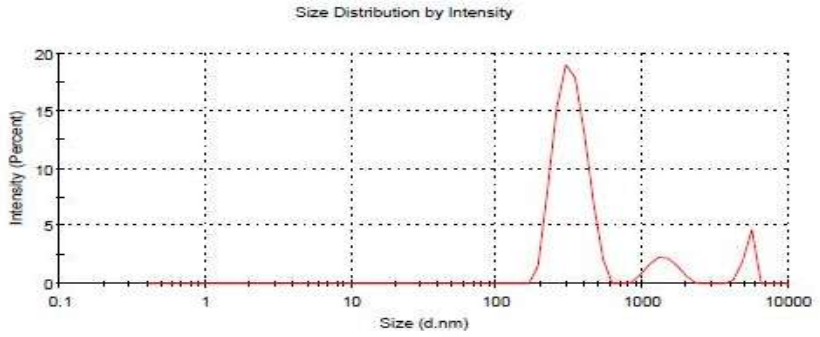

(b)

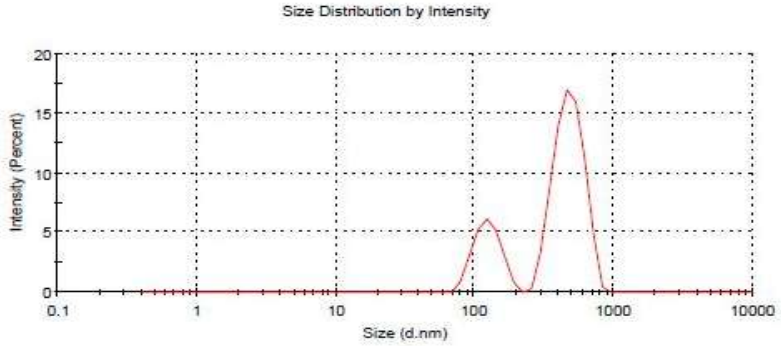

(c)

Figure 23. Size distribution of (a) synthesized HAp (b) calcined HAp at 850°C and (c) calcined HAp at 1200°C

4.3 Micro-hardness of all CP-Ti samples

Micro-hardness of CP-Ti samples has been increased after microwave processing. The reason behind of increased microhardness is due to formation of rutile (TiO_2) phase along with hydroxyapatite particles. For TiO_2- HAp composite coated CP-Ti samples, approx 20 HV hardness increased from unfuntionalized samples has been recorded (**Figure 24.**). There is no significant difference of hardness observed between synthesized HAp and calcined

HAp coated CP-Ti samples. So, titanium oxide formation on titanium surface would be the prime factor for increasing hardness.

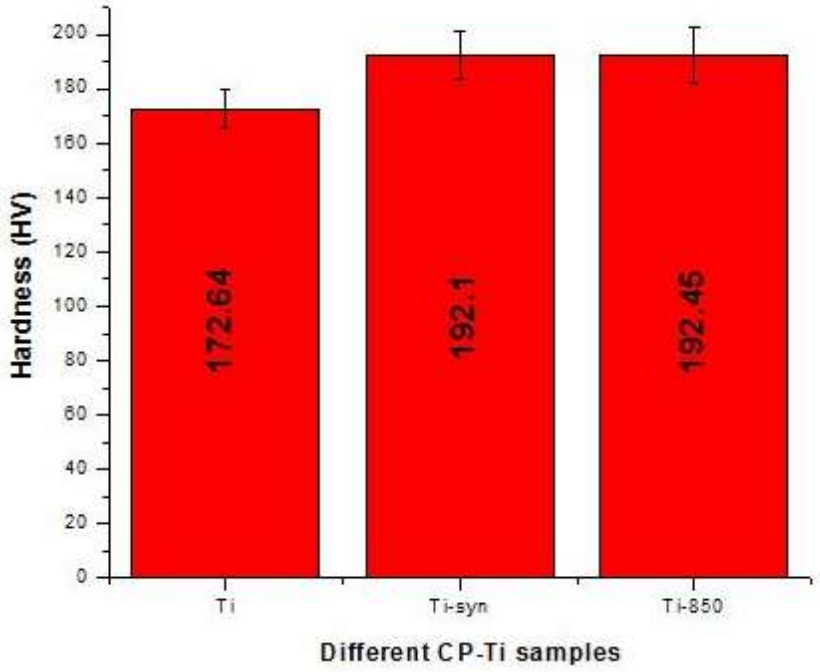

Figure 24. Microhardness of different CP-Ti samples

4.4 Protein adsorption studies

Different proteins adsorbed on the surface of an implant mediate its further biological responses such as cell attachment and proliferation. The chemistry, roughness, and charge of the CP-Ti surfaces play an important role on the adsorption of proteins. In this study, it is seen that uncoated specimens have higher values of absorbance. Absorbance is directly proportional to the concentration of an element (from Beer-Lambert Law). So, higher absorbance means a lower amount of protein adsorption. Total amount of the protein adsorption for individual CP-Ti samples were calculated by standard curve. In this study, it is seen that the least amount of protein was adsorbed on the uncoated CP-Ti specimen. The amount of adsorbed BSA had increased in the sequence of 850°C calcined HAp(ti850) > synthesized HAp(tiS) > uncoated CP-Ti (ti) specimens (**Figure 25**.). A highly significant increase was observed in protein adsorption of calcined HAp coated specimens, whereas, synthesized HAp coated specimens showed an insignificant increase when compared to uncoated CP-Ti. The adsorption of protein on the titania-HAp coated CP-Ti surface is highly influenced by the occurrence of hydrophilic functional groups. The absence of such functional groups on uncoated CP-Ti has led to minimum protein adsorption.

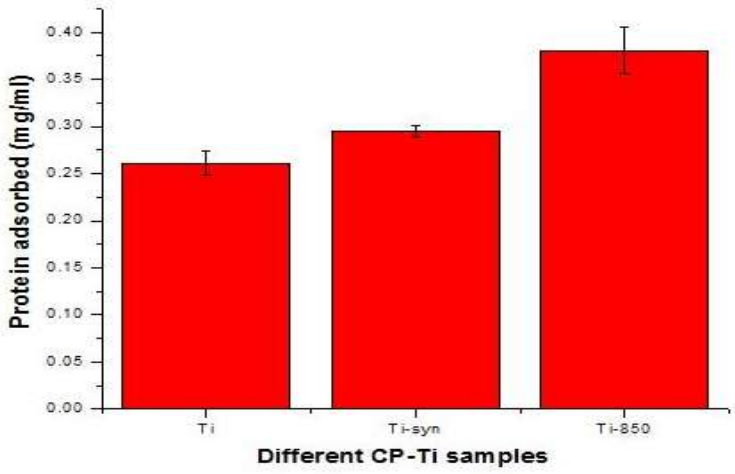

Figure 25. Protein adsorption studies of different CP-Ti samples after 24h

4.5 Hemocompatibility studies

One of the most important *in vitro* properties of implants is their hemocompatibility. The implant has to be in contact with blood for a long period and during this period their interaction may lead to cell damage and blood clotting. So it is essential to study the interaction of blood components with implant material. The hemolysis percentage of the various cpTi specimens showed in **Figure 26.**. All the coated CP-Ti specimens showed their hemocompatibility in nature. The increase in haemolytic nature was seen in the order of Ti-850°C < coated Ti-syn < CP-Ti (Fig. 25.). 850°C calcined HAp samples presented high significant decrease in hemolysis percentage.

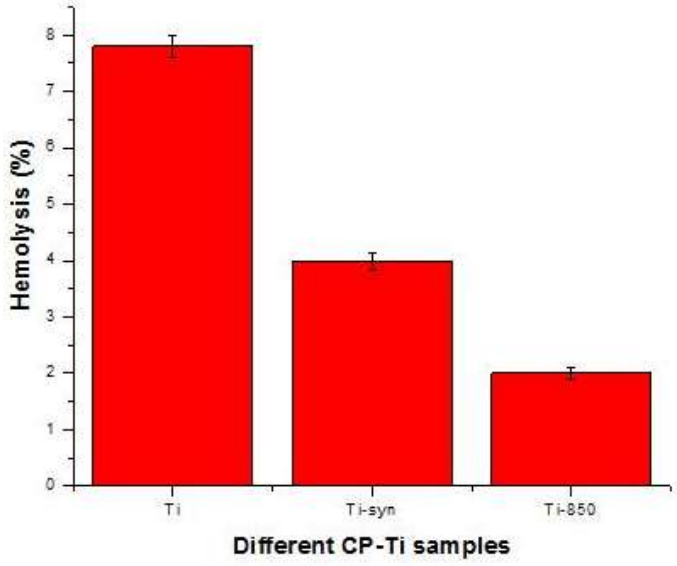

Figure 26. Percentage hemolysis of different CP-Ti specimens after incubation time of 1 hr

4.6 Bioactivity studies

The CP-Ti specimens were analysed for their *in vitro* bioactivity study by immersing them in SBF solution in a water bath for 21 days. Apatite formations were analysed by using SEM. Morphologies of unfuntionalized and funtionalized CP-Ti were characterized by using FESEM (**Figure 27.**) confirmed the formation of apatite on the surface of the various CP-Ti specimens. Total amount of apatite formation on the surfaces of the composites were quantified by EDS analysis. The percentage of elemental composition of apatite was given in following tables for all CP-Ti samples. Amount of apatite formation were increased in the order of uncoated CP-Ti < synthesized HAp coated CP-Ti < calcined (850°C) HAp coated CP-Ti. Apatite formation is more favourable in calcined HAp coated titanium. This is because calcined HAp sample has more crystalline in nature which is closed to bone inorganic element. So, calcined HAp coated sample is more bioactive than synthesized HAp coated sample.

(a)

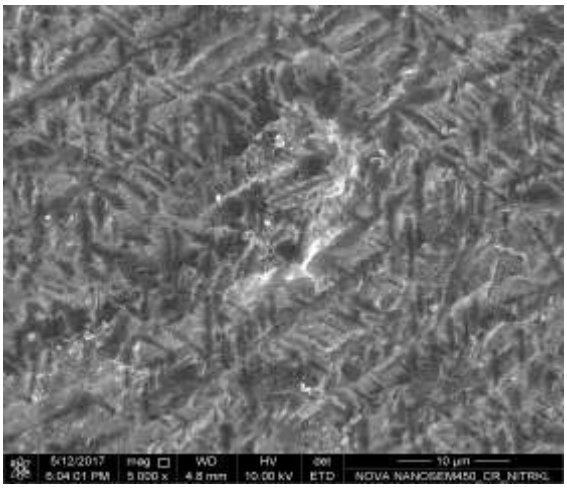

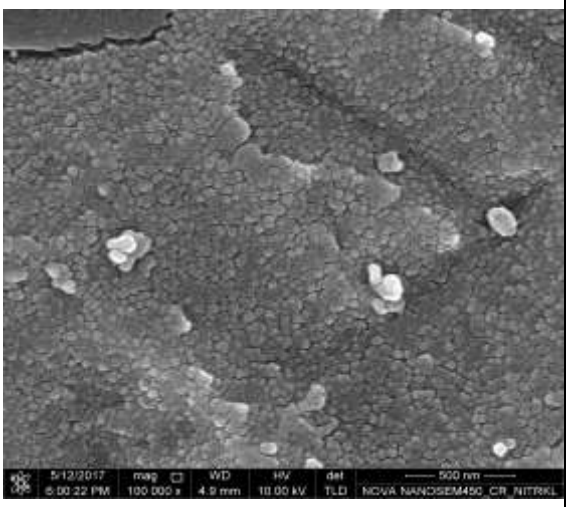

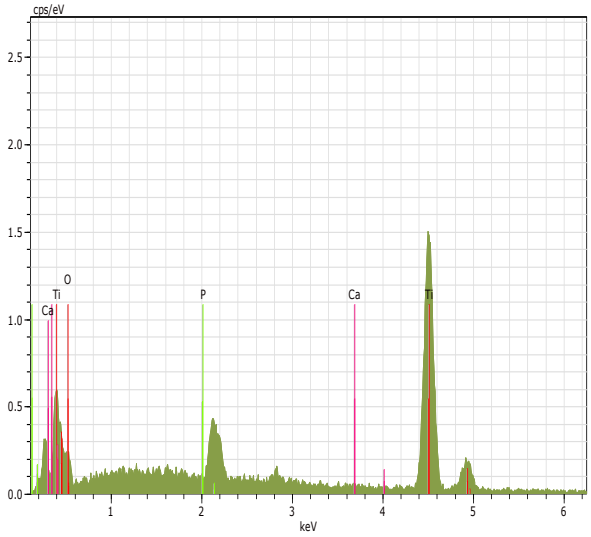

Element	At %
O	20.57
P	0.16
Ca	0.53
Ti	78.74

(b)

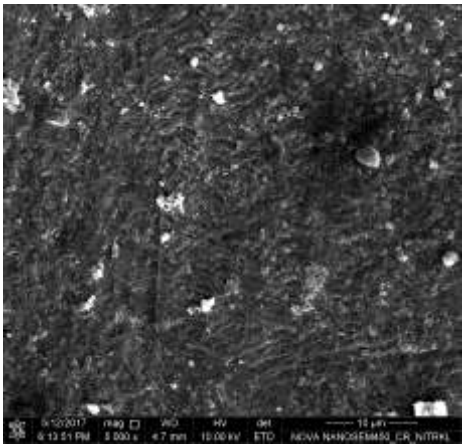

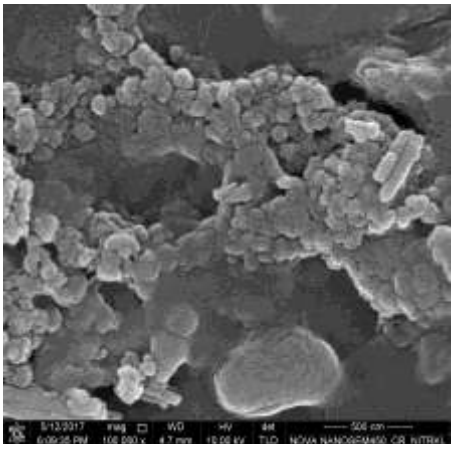

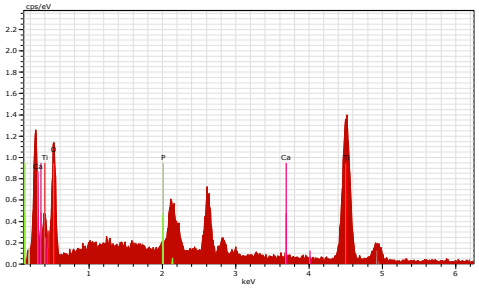

Element	At %
O	55.34
P	0.24
Ca	1.08
Ti	43.34

(c)

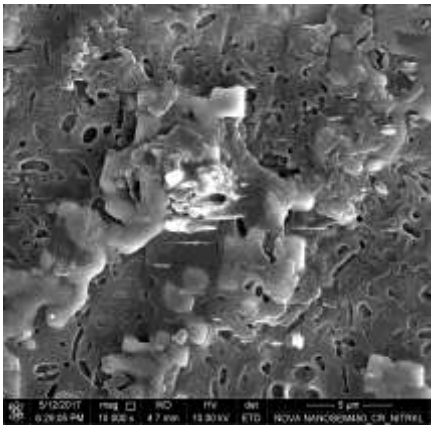

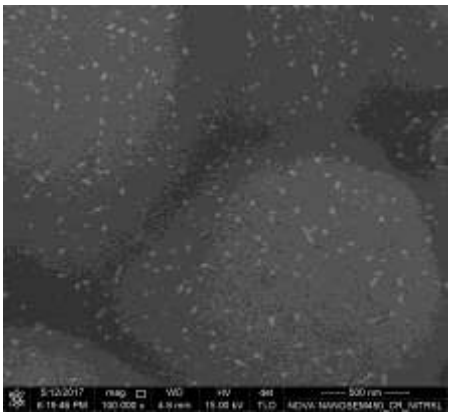

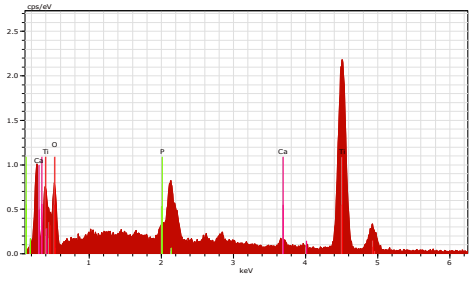

Element	At %
O	35.51
P	1.02
Ca	1.57
Ti	61.89

Figure 27. FESEM images and EDS analysis of (a) uncoated CP-Ti, (b) synthesized HAp coated CP-Ti, and (c) calcined (850°C) HAp coated CP-Ti sample after bioactivity test at different magnifications

4.7 Cell viability assay

Cell proliferation is an indicator of osteogenic activity of osteoblast cells. The ability of any biomaterial to promote cell proliferation is important for osseointegration. MG 63 cell line, an established model for human osteoblasts was used to study the response of osteoblast cells on the functionalized cpTi specimens by performing MTT assay and the results are shown in **Figure 28.** Amongst all the specimens, uncoated CP-Ti shows the least cell viability. The coated CP-Ti has lead to an increased cell viability of the order of uncoated CP-Ti < synthesized HAp coated CP-Ti < calcined HAp (850°C). This result correlates with above all biological studies.

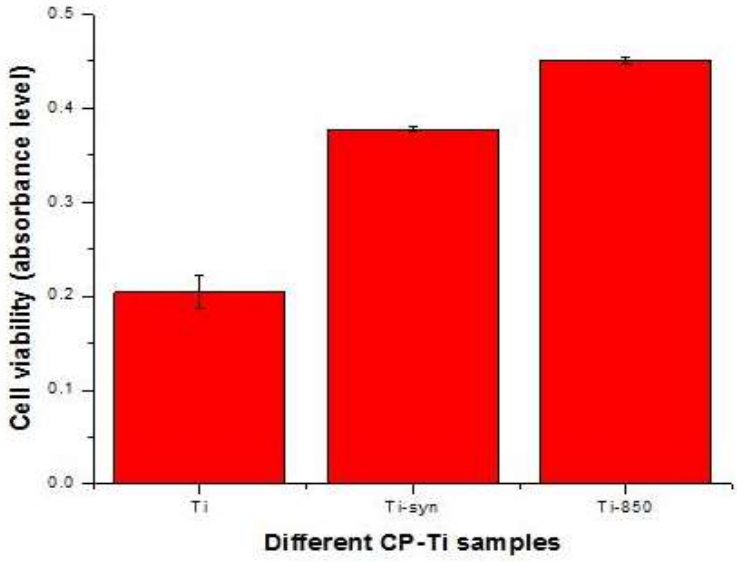

Figure 28. Cell viability results of different CP-Ti specimens after 48 h of cell seeding

Chapter 4

Conclusion

Hydroxyapatite (HAp) was prepared by the wet chemical method, and characterized using XRD, and FT-IR. After preparing HAp sample, calcination or heat treatment of HAp was done at 850°C and 1200 °C for 2 h. The requirement of calcination is to the reduction of structure's water and increases the degree of crystallinity. It is concluded that, calcined HAp is more pure and crystalline than synthesized HAp. The synthesized HAp has favourable thermal stability at 1200 °C. From zeta potential analysis, we can infer that the HAp particles are not stable in colloidal form. Their tendency is to flocculate in a suspension. From DLS data, it is inferred that an increase in temperature had a slight effect on particle size-; particle sizes increased due to sintering. Calcined and synthesized HAp were characterized by XRD, FTIR, SEM, and EDS analysis. The 850°C calcined HAp samples were considered more suitable than calcined HAp rather than 1200°C calcined HAp due to its Ca/P ratio. By microwave processing, composite of coating of HAp-titania were formed and confirmed by XRD analysis. Titanium oxide layer formed on titanium substrate during microwave processing and hydroxyapatite sintered along with oxide layer. Mechanical properties of CP-Ti altered due to incorporating titanium oxide layer, hardness of the material increased due to TiO_2 layer. Four biological studies were done for evaluating biological performances of HAp coated samples. Due to highly bioactive, and osteoconductive in nature, HAp coated samples are more suitable for bone ingrowth and osteointegration. Porous nature of HAp coating has been found in SEM analysis, which is more favourable for protein adherence and bone ingrowth. From these studies, it can be concluded that calcined HAp (at 850°C) samples are more beneficial for coating on titanium rather than synthesized HAp sample.

Future scope

- Determine the stoichiometric or non-stoichiometric oxide layer formation during Microwave processing
- Contact angle measurement of coated and uncoated CP-Ti sample.
- Measurement of surface roughness, and determine the relationship between surface roughness and hardness.
- Comparative analysis of all the HAp samples by TEM.

References

[1] Long, Marc, and H. J. Rack. "Titanium alloys in total joint replacement—a materials science perspective." *Biomaterials* 19, no. 18 (1998): 1621-1639.

[2] de Jonge, Lise T., Sander CG Leeuwenburgh, Joop GC Wolke, and John A. Jansen. "Organic–inorganic surface modifications for titanium implant surfaces." *Pharmaceutical research* 25, no. 10 (2008): 2357-2369.

[3] Buser, D., R. K. Schenk, S. Steinemann, J. P. Fiorellini, C. H. Fox, and H. Stich. "Influence of surface characteristics on bone integration of titanium implants. A histomorphometric study in miniature pigs." *Journal of biomedical materials research* 25, no. 7 (1991): 889-902.

[4] Webster, Thomas J., and Jeremiah U. Ejiofor. "Increased osteoblast adhesion on nanophase metals: Ti, Ti6Al4V, and CoCrMo." *Biomaterials* 25, no. 19 (2004): 4731-4739.

[5] Hench, Larry L. "Bioceramics: from concept to clinic." *Journal of the american ceramic society* 74, no. 7 (1991): 1487-1510.

[6] Song, Ho-Jun, Seong-Hwan Park, Sang-Hun Jeong, and Yeong-Joon Park. "Surface characteristics and bioactivity of oxide films formed by anodic spark oxidation on titanium in different electrolytes." *Journal of Materials Processing Technology* 209, no. 2 (2009): 864-870.

[7] Schuler, Martin, Diana Trentin, Marcus Textor, and Samuele GP Tosatti. "Biomedical interfaces: titanium surface technology for implants and cell carriers." *Nanomedicine* 1, no. 4 (2006): 449-463.

[8] Narayanan, R., S. K. Seshadri, T. Y. Kwon, and K. H. Kim. "Calcium phosphate-based coatings on titanium and its alloys." *Journal of Biomedical Materials Research Part B: Applied Biomaterials* 85, no. 1 (2008): 279-299.

[9] Burgess, Ann V., Brooks J. Story, Danny La, William R. Wagner, and John P. LeGeros. "Highly crystalline MP-1 hydroxylapatite coating Part I: In vitro characterization and comparison to other plasma-sprayed hydroxylapatite coatings." *Clinical oral implants research* 10, no. 4 (1999): 245-256.

[10] Siddharthan, A., TS Sampath Kumar, and S. K. Seshadri. "In situ composite coating of titania–hydroxyapatite on commercially pure titanium by microwave processing." *Surface and Coatings Technology* 204, no. 11 (2010): 1755-1763.

[11] Cook, Stephen D., Kevin A. Thomas, John F. Kay, and Michael Jarcho. "Hydroxyapatite-coated titanium for orthopedic implant applications." *Clinical orthopaedics and related research* 232, (1988): 225-243.

[12] Sokolova, Viktoriya, Diana Kozlova, Torben Knuschke, Jan Buer, Astrid M. Westendorf, and Matthias Epple. "Mechanism of the uptake of cationic and anionic calcium phosphate nanoparticles by cells." *Acta biomaterialia* 9, no. 7 (2013): 7527-7535.

[13] Sadat-Shojai, Mehdi, Mohammad-Taghi Khorasani, Ehsan Dinpanah-Khoshdargi, and Ahmad Jamshidi. "Synthesis methods for nanosized hydroxyapatite with diverse structures." *Acta biomaterialia* 9, no. 8 (2013): 7591-7621.

[14] Koutsopoulos, Synthesis. "Synthesis and characterization of hydroxyapatite crystals: a review study on the analytical methods." *Journal of biomedical materials research* 62, no. 4 (2002): 600-612.

[15] Iafisco, Michele, Elena Varoni, Elisa Battistella, Stefano Pietronave, Maria Prat, Norberto Roveri, and Lia Rimondini. "The cooperative effect of size and crystallinity degree on the resorption of biomimetic hydroxyapatite for soft tissue augmentation." *International Journal of Artificial Organs* 33, no. 11 (2010): 765-774

[16] Chen, Fei, Zhou-Cheng Wang, and Chang-Jian Lin. "Preparation and characterization of nano-sized hydroxyapatite particles and hydroxyapatite/chitosan nano-composite for use in biomedical materials." *Materials letters* 57, no. 4 (2002): 858-861.

[17] Uskoković, Vuk, and Dragan P. Uskoković. "Nanosized hydroxyapatite and other calcium phosphates: chemistry of formation and application as drug and gene delivery agents." *Journal of biomedical materials research Part B: Applied biomaterials* 96, no. 1 (2011): 152-191.

[18] Garcia-Sanz, F. J., M. B. Mayor, J. L. Arias, J. Pou, B. Leon, and M. Perez-Amor. "Hydroxyapatite coatings: a comparative study between plasma-spray and pulsed laser deposition techniques." *Journal of Materials Science: Materials in Medicine* 8, no. 12 (1997): 861-865.

[19] Sadat-Shojai, Mehdi, Mohammad-Taghi Khorasani, Ehsan Dinpanah-Khoshdargi, and Ahmad Jamshidi. "Synthesis methods for nanosized hydroxyapatite with diverse structures." *Acta biomaterialia* 9, no. 8 (2013): 7591-7621.

[20] Chouksey, Ashish Kumar, Hemlata Bundela, Vishal Bhardwaj, and Deepika Garg. "Preparation and Characterization of Nano Size Hydroxyapatite Powder (n-HAp): Study of Swelling Behavior for its perspective use in various Biological Applications."

[21] Santos, Maria Helena, Marise de Oliveira, Luciana Palhares de Freitas Souza, Herman Sander Mansur, and Wander Luiz Vasconcelos. "Synthesis control and characterization of hydroxyapatite prepared by wet precipitation process." *Materials Research* 7, no. 4 (2004): 625-630.

[22] Santos, Maria Helena, Marise de Oliveira, Luciana Palhares de Freitas Souza, Herman Sander Mansur, and Wander Luiz Vasconcelos. "Synthesis control and characterization of hydroxyapatite prepared by wet precipitation process." *Materials Research* 7, no. 4 (2004): 625-630.

[23] Santos, Maria Helena, Marise de Oliveira, Luciana Palhares de Freitas Souza, Herman Sander Mansur, and Wander Luiz Vasconcelos. "Synthesis control and characterization of hydroxyapatite prepared by wet precipitation process." *Materials Research* 7, no. 4 (2004): 625-630.

[24] Suchanek, Wojciech L., and Richard E. Riman. "Hydrothermal synthesis of advanced ceramic powders." In *Advances in Science and Technology*, vol. 45, pp. 184-193. Trans Tech Publications, 2006.

[25] Sadat-Shojai, M. "Preparation of hydroxyapatite nanoparticles: comparison between hydrothermal and solvo-treatment processes and colloidal stability of produced nanoparticles in a dilute experimental dental adhesive." *J Iran Chem Soc* 6, no. 2 (2009): 386-392.

[26] Manafi, Saheb Ali, and Sedigheh Joughehdoust. "Synthesis of hydroxyapatite nanostructure by hydrothermal condition for biomedical application." *Iranian Journal of Pharmaceutical Sciences* 5, no. 2 (2009): 89-94.

[27] Thamaraiselvi, T. V., K. Prabakaran, and S. Rajeswari. "Synthesis of hydroxyapatite that mimic bone minerology." *Trends Biomater Artif Organs* 19, no. 2 (2006): 81-83.

[28] Kokubo, Tadashi, and Hiroaki Takadama. "How useful is SBF in predicting in vivo bone bioactivity?." *Biomaterials* 27, no. 15 (2006): 2907-2915.

[29] Manso, Miguel, Carmen Jimenez, Carmen Morant, Pilar Herrero, and J. M. Martınez-Duart. "Electrodeposition of hydroxyapatite coatings in basic conditions." *Biomaterials* 21, no. 17 (2000): 1755-1761.

[30] Gergely, Gréta, Ferenc Wéber, István Lukács, Attila L. Tóth, Zsolt E. Horváth, Judit Mihály, and Csaba Balázsi. "Preparation and characterization of hydroxyapatite from eggshell." *Ceramics International* 36, no. 2 (2010): 803-806.

[31] Cho, Dong-Woo, Jin Woo Lee, Jong Young Kim, and Tae-Yun Kang. "Solid freeform fabrication method applied to tissue scaffolds." In *Handbook of Intelligent Scaffold for Tissue Engineering and Regenerative Medicine*, pp. 609-631. Pan Stanford Publishing, 2012.

[32] Hench, Larry L. "Bioceramics: from concept to clinic." *Journal of the american ceramic society* 74, no. 7 (1991): 1487-1510.

[33] Hawryluk, R. J., D. J. Campbell, G. Janeschitz, P. R. Thomas, R. Albanese, R. Ambrosino, C. Bachmann et al. "Principal physics developments evaluated in the ITER design review." *Nuclear Fusion* 49, no. 6 (2009): 065012.

[34] Zhou, Hongjian, and Jaebeom Lee. "Nanoscale hydroxyapatite particles for bone tissue engineering." *Acta biomaterialia* 7, no. 7 (2011): 2769-2781.

[35] López-Macipe, Anabel, Jaime Gómez-Morales, and Rafael Rodríguez-Clemente. "Nanosized hydroxyapatite precipitation from homogeneous calcium/citrate/phosphate solutions using microwave and conventional heating." *Advanced Materials* 10, no. 1 (1998): 49-53.

[36] Park, Joon, and Roderic S. Lakes. *Biomaterials: an introduction*. Springer Science & Business Media, 2007.

[37] Mucalo, Michael, ed. *Hydroxyapatite (HAp) for biomedical applications*. Elsevier, 2015.

[38] Mishra, Radha Raman, and Apurbba Kumar Sharma. "Microwave–material interaction phenomena: heating mechanisms, challenges and opportunities in material processing." *Composites Part A: Applied Science and Manufacturing* 81 (2016): 78-97.

[39] Bradshaw, S. M., E. J. Van Wyk, and J. B. De Swardt. "Microwave heating principles and the application to the regeneration of granular activated carbon." *Journal of the South African Institute of Mining and Metallurgy(South Africa)* 98, no. 4 (1998): 201-210.

[40] Rodríguez-Clemente, R., A. López-Macipe, J. Gómez-Morales, J. Torrent-Burgués, and V. M. Castano. "Hydroxyapatite precipitation: a case of nucleation-aggregation-agglomeration-growth mechanism." *Journal of the European Ceramic Society* 18, no. 9 (1998): 1351-1356.

[41] Harada, Yoshitada, Jeng-Tzung Wang, Vivek A. Doppalapudi, Andrew A. Willis, Murali Jasty, William H. Harris, Mitsuo Nagase, and Steven R. Goldring. "Differential effects of different forms of hydroxyapatite and hydroxyapatite/tricalcium phosphate particulates on human monocyte/macrophages in vitro." *Journal of Biomedical Materials Research Part A* 31, no. 1 (1996): 19-26.

[42] D'antonio, James A., William N. Capello, Michael T. Manley, Rudolph GT Geesink, and William L. Jaffe. "Hydroxyapatite femoral stems for total hip arthroplasty: 10–14 year follow-up." In *Fifteen Years of Clinical Experience with Hydroxyapatite Coatings in Joint Arthroplasty*, pp. 235-241. Springer Paris, 2004.

[43] Koutsopoulos, Synthesis. "Synthesis and characterization of hydroxyapatite crystals: a review study on the analytical methods." *Journal of biomedical materials research* 62, no. 4 (2002): 600-612.

[44] Prokopiev, Oleg, and Igor Sevostianov. "Dependence of the mechanical properties of sintered hydroxyapatite on the sintering temperature." *Materials Science and Engineering: A* 431, no. 1 (2006): 218-227.

[45] Rodríguez-Clemente, R., A. López-Macipe, J. Gómez-Morales, J. Torrent-Burgués, and V. M. Castano. "Hydroxyapatite precipitation: a case of nucleation-aggregation-agglomeration-growth mechanism." *Journal of the European Ceramic Society* 18, no. 9 (1998): 1351-1356.

[46] Clogston, Jeffrey D., and Anil K. Patri. "Zeta potential measurement." *Characterization of nanoparticles intended for drug delivery* (2011): 63-70.

[47] Bhattacharjee, Sourav. "DLS and zeta potential–What they are and what they are not?." *Journal of Controlled Release* 235 (2016): 337-351.